LAPPEENRANTA UNIVERSITY OF TECHNOLOGY
DEPARTMENT OF ENERGY AND ENVIRONMENTAL TECHNOLOGY

WAVELET ANALYSIS IN TURBULENCE

The Departmental Council approved the subject of this Thesis for the Degree of Master of Science on the 9th June 2004.

Supervisor: Professor Pertti Sarkomaa
Instructor: Dr. Tech. Payman Jalali

Lappeenranta 14th October 2004

Päivi Sikiö
Kesselintie 82
56440 Pohja-Lankila
050-5564303

ABSTRACT

Lappeenranta University of Technology

Department of Energy and Environmental Technology

Sikiö, Päivi

Wavelet Analysis in Turbulence

Master's Thesis

2004

60 pages, 25 figures and 4 tables.

Examiners: Professor Pertti Sarkomaa

Dr. Tech. Payman Jalali

Keywords: wavelet, wavelet transform, turbulence model, shell model

The objective of this thesis is to study wavelets and their role in turbulence applications. Under scrutiny in the thesis is the intermittency in turbulence models. Wavelets are used as a mathematical tool to study the intermittent activities that turbulence models produce.

The first section generally introduces wavelets and wavelet transforms as a mathematical tool. Moreover, the basic properties of turbulence are discussed and classical methods for modeling turbulent flows are explained. Wavelets are implemented to model the turbulence as well as to analyze turbulent signals.

The model studied here is the GOY (Gledzer 1973, Ohkitani & Yamada 1989) shell model of turbulence, which is a popular model for explaining intermittency based on the cascade of kinetic energy. The goal is to introduce better quantification method for intermittency obtained in a shell model. Wavelets are localized in both space (time) and scale, therefore, they are suitable candidates for the study of singular bursts, that interrupt the calm periods of an energy flow through various scales. The study concerns two questions, namely the frequency of the occurrence as well as the intensity of the singular bursts at various Reynolds numbers.

The results gave an insight that singularities become more local as Reynolds number increases. The singularities become more local also when the shell number is increased at certain Reynolds number. The study revealed that the singular bursts are more frequent at $Re \sim 10^7$ than other cases with lower Re. The intermittency of bursts for the cases with $Re \sim 10^6$ and $Re \sim 10^5$ was similar, but for the case with $Re \sim 10^4$ bursts occured after long waiting time in a different fashion so that it could not be scaled with higher Re.

TIIVISTELMÄ

Lappeenrannan teknillinen yliopisto

Energia ja ympäristötekniikan osasto

Sikiö, Päivi

Turbulenttisen signaalin väreanalyysi

Diplomityö

2004

60 sivua, 25 kuvaa ja 4 taulukkoa

Tarkastajat: Professori Pertti Sarkomaa

Tekn. Tohtori Payman Jalali

Hakusanat: väre, väreanalyysi, aalloke, wavelet-muunnos, turbulenssi, turbulenssimalli

Tämän työn tavoitteena on tutustua väreisiin ja niiden käyttöön turbulenttisen virtauksen sovelluksissa. Tutkimuksen kohteena tässä työssä on ajoittaisuus turbulenssimallin tuottamassa signaalissa. Turbulenttisessa virtauksessa ajoittaisuus aiheutuu yksittäisistä turbulenttisista purkauksista hiljaisten jaksojen välillä. Matemaattisena menetelmänä signaalissa esiintyvien dissipaatiopiikkien tutkimisessa käytetään väreanalyysiä.

Teoriaosassa käsitellään väreitä ja väreanalyysiä sekä perehdytään turbulenssin perusominaisuuksiin. Tarkoituksena on myös esitellä ja vertailla erilaisia tapoja mallintaa turbulenssia. Teoriaosuudessa tutustutaan väreiden käyttöön turbulenssin mallinnuksessa ja analysoinnissa.

Työssä tutkittu turbulenssisovellus on GOY (Gledzer 1973, Ohkitani & Yamada 1989) shell-malli, jota käytetään yleisesti selittämään turbulenssin ajoittaisuutta. Tutkimuksen kohteena on shell-mallin tuottaman dissipaatiosignaalin ajoittaisuus. Väreet sopivat tähän tutkimukseen hyvin niiden aika- ja skaala-lokalisaation johdosta. Tutkimuksessa keskityttiin erityisesti kahteen kysymykseen: dissipaatiopurkausten singulaarisuuteen sekä niiden esiintymistiheyteen.

Tutkimus osoitti, että dissipaatiopurkaukset muuttuvat paikallisemmiksi, kun Reynoldsin lukua kasvatetaan. Samoin tapahtuu, jos shell-lukua kasvatetaan tietyllä Reynoldsin luvulla. Dissipaatiopurkausten esiintymistiheys on suurin, kun Reynoldsin luku on $Re \sim 10^7$. Reynoldsin luvuilla $Re \sim 10^6$ ja $Re \sim 10^5$ purkausten esiintymistiheys on samaa luokkaa. Reynoldsin luvulla $Re \sim 10^4$ purkausten väli kasvaa niin suureksi, että skaalaus korkeampien Reynoldsin luvun tapausten kanssa on vaikeaa.

ACKOWLEDGEMENTS

I wish to express my sincere thanks to Professor Pertti Sarkomaa and Dr. Tech. Payman Jalali for their supervision and guidance. Their support and encouragement has been invaluable to me during my studies at Lappeenranta University of Technology.

I would also like to thank all the personel of the Department of Energy and Environmental Technology for the kind assistance and good working environment they provided. Especially I want to thank Jouni Ritvanen, Tero Tynjälä and Anne Jordan for their support, encouragement and friendship.

I want to express my gratitude to my parents Hilkka and Seppo Särelä for their understanding, care and attention. Finally I want to give my special thanks to my husband Yrjö and my children Joni and Henna – they gave me the drive and determination to reach my goal.

This study was funded by the Academy of Finland.

Lappeenranta 14th October 2004

Päivi Sikiö

TABLE OF CONTENTS

NOMENCLATURE

Latin letters

a	scale parameter [-]
a^*	normalized scale [-]
A	coefficient [-]
b	translation parameter [-]
f	force [N]
f^*	normalized frequency [-]
F	force [N]
g	window function [-]
k	wave number [-]
K	reproducing kernel [-]
l	length [m]
L	scale [-]
m	integer part of dilation [-]
n	integer part of transition [-]
N	number of shells [-]
N_d	number of data points in signal [-]
q	scaling factor [-]
Re	Reynolds number [-]
t	time [s]
T	energy exchange rate [m^2/s^3]
s	strain-rate tensor [-]
u	velocity [m/s]
V	velocity [m/s]
x	x-coordinate [m]
y	y-coordinate [m]
z	z-coordinate [m]
Z	partition function [-]

Greek letters

α	local scaling exponent [-]
β	integer exponent [-]
ε	dissipation rate [-]
η	porosity [-]
ν	dimensionless kinematic viscosity [-]
τ	incoherent stress [-]
τ_q	partition function scaling exponent [-]
ϕ	scaling function [-]
χ	masc function [-]
ψ	wavelet function [-]
ω	frequency [1/s]
ω	vorticity [-]

Subscripts

a	active
C	coherent
I	incoherent
J	index
l	developed stage
m	mean
n	index
s	prestage

Superscripts

^	transform
–	mean
*	complex conjugate
μ	index

’ nearest neighbor

” next nearest neighbor

Abbreviations

2-D	two dimensional
3-D	three dimensional
CVS	coherent vortex simulation
CWT	continuous wavelet transform
DNS	direct numerical simulation
DWT	discrete wavelet transform
GOY	Gledzer - Ohkitani - Yamada
LES	Large-Eddy Simulations
MRA	multiresolution analysis
PDF	probability distribution function
RANS	Reynolds Averaged Navier-Stokes
URANS	Unsteady Reynolds Averaged Navier-Stokes
WT	Wavelet transform

1 INTRODUCTION

One of the most interesting problems in fluid engineering is the study of turbulent flows. The analysis of turbulent flow field is much more complicated than that of laminar flows. All classical spectral methods to handle turbulence rely on the Fourier representation. The ordinary Fourier transform maps the function from time space to frequency space but the time-localization information of the signal is lost. Turbulent flows consist of two parts, coherent structures and incoherent background flow. The size and spatial distribution of coherent structures are in key position in understanding turbulence but space-scale analysis is not possible with Fourier transformation. A more appropriate tool is needed.

Wavelets are the basis functions which are localized in both space and scale and they can express the frequency category of a signal at a given time or position. Wavelet transform is performed locally on the signal and the formations and collapses of special structures in a signal can be identified. The time-frequency localization characteristic of wavelet transform enables the detection of the locations of singularities and discontinuities in a signal, which is impossible with ordinary Fourier analysis.

The objective of this thesis is to introduce wavelets and wavelet transforms as a mathematical tool especially in applications for turbulence. The properties of turbulence and turbulence modeling are discussed generally and wavelets are proposed to model and analyze turbulence. The application under study in the thesis is the intermittency in a turbulence model. Wavelets are used to investigate the intermittent activities that the model produces.

The turbulence model studied here is the GOY (Gledzer 1973, Ohkitani & Yamada 1989) shell model. It is generally used for explaining turbulent intermittency. The goal of this work is to quantify the intermittency that the model produces more precisely. Simulations are performed with varying Reynolds number, shell number and external forcing. Then the properties of singular bursts appeared in energy

dissipation signal are studied through different cases using continuous wavelet transform.

2 WAVELETS AS A MATHEMATICAL TOOL

2.1 General

Wavelets and wavelet transforms are relatively recent developments in applied mathematics. They are based on group theory and square integrable representations and they provide a tool for many engineering fields starting from signal processing, image coding and numerical analysis. The advantage of this method compared to other existing methods is the possibility to expand a signal, or a field, into both space and scale, and perhaps directions.

In many applications there is a signal and one is interested in its frequency content in time. With Fourier transform it is possible to get a representation of the frequency content of the signal but the time-localization of frequency cannot be read from it. Wavelets are localized in space and frequency, therefore wavelet transform analyzes a signal locally in space and frequency domains.

The time-frequency localization characteristic of wavelet transform gives a great possibility to detect the locations of singularities and discontinuities in a signal, which is impossible to achieve in ordinary Fourier analysis. Wavelets are also better suited for de-noising and compressing purposes than other methods. Additional interesting applications of wavelets can be found in function approximation, neutral network systems, solving partial differential equations and analysis of turbulence in fluid mechanics.

2.2 History of wavelets

From historical point of view, wavelet theory is a new and rapidly evolving technique. Its mathematical groundwork was done in the nineteenth century, when Joseph Fourier worked out his theories of frequency analysis. Wavelets were developed from that base to provide a tool for time-frequency localization.

The first known wavelet is Haar, with a basis laid in 1909 by Alfred Haar. Though the wavelet transform itself was first proposed not until in 1980 by Jean Morlet, a scientist working on seismic data analysis, and the team of Alex Grossmanns at the Marseille Theoretical Physics Center in France. Morlet and Grossmann developed the geometrical formalism of the continuous wavelet transform and in 1985 it was extended to *n* dimensions by Y. Meyer, who mainly developed the methods of wavelet analysis with his colleagues.

The continuous wavelet transform is a good tool for analyzing the local differentiability of a function and for detecting and characterizing its singularities. The work on this subject was set in motion by Holschneider, Jaffard, Arnéodo, Tchamitchian, Mallat and Hwang in 1988 – 1991. The continuous wavelet transform was also found to be useful tool for signal processing, especially with the skeleton technique. The study of this area was started by Escudié, Torresani, Tchamitchian and Delprat in 1989 – 1991.

The discrete wavelet transform was created by Meyer, Grossmann and Daubechies in 1986. They selected a discrete subset, “a wavelet frame”, of the continuous wavelet space so that it constitutes a quasi-orthogonal complete set. In addition to this Grossmann and Morlet had earlier discovered that it is possible to recompute the whole set of the continuous wavelet coefficients from a discrete subset of the wavelet coefficients. It can be done using an interpolation formula that is based on the reproducing kernel property of the continuous wavelet transform.

In 1986 Meyer was trying to prove that there could not be a true orthogonal basis constructed with regular wavelets and therefore he was supprised to find such an orthogonal basis built from a regular wavelet. In collaboration with his student Lemarié he then extended it to the *n*-dimensional case. In 1987 Meyer and Mallat proposed the concept of multiresolution analysis which gives a general method for building orthogonal wavelet bases and leads to the implementation of fast wavelet algorithms.

Since nineties the wavelet domain has been growing rapidly, because of the great variety of possible applications. Already wavelets have been succesfully used for example in signal processing, image coding and numerical analysis and further development is being done all the time. The majour work with wavelets on a field of turbulence has been done in recent years by Marie Farge. [1, 2]

2.3 Wavelet transform compared with Fourier Transform

2.3.1 The standard Fourier Transform

The standard Fourier transform is defined using the continuous integration of the product of a function *f(t)* by the trigonometric functions and it can be written as

$$\hat{f}(\omega) = \frac{1}{\sqrt{2\pi}} \int_{-\infty}^{+\infty} f(t) e^{-i\omega t} dt \,, \tag{1}$$

where ω is frequency and t is time.

Fourier transform maps a function from time domain to frequency domain. Any function can be decomposed into a linear combination of Fourier vectors defined by their Fourier coefficients $\hat{f}(\omega)$. However for trigonometric functions it is characteristic to oscillate forever, so the information of *f(t)* is completely delocalized among the spectral coefficients $\hat{f}(\omega)$. Standard Fourier transform does not therefore provide any information of time-localization but it is an appropriate tool for frequency analysis and when studying harmonic or stationary signals or when there is no need for local information. [1, 2, 3]

2.3.2 Windowed Fourier transform

Often there is non-stationary or transitory characteristics, such as abrupt changes or beginnings and endings of events, in the signal. With the ordinary Fourier transform it is not possible to analyze when the singular event occurred. Using windowed

Fourier transform some degree of time-localization can be achieved. The windowed Fourier transform is defined by

$$\hat{f}_{\mathrm{w}}(\omega,t) = \int_{-\infty}^{+\infty} f(t)g(t-t_0)e^{-i\omega t}\,dt\,, \tag{2}$$

where $g(t-t_0)$ represents window function.

The function $f(t)$ is multiplied by the window function $g(t-t_0)$ to cut off a well-localized slice of f, like shown in figure 1.

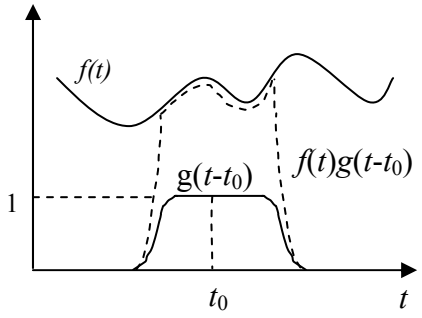

Figure 1. The windowed Fourier transform. [1]

The window function is then shifted along the time axis (by changing t_0) and the Fourier transform is performed to get a description of f in the time-frequency plane.

Though this method is a standard technique, it has its disadvantages. Namely the size of the time window, once chosen, can not be changed during the analysis. This means that the window is same for all frequencies. If the window could be varied during the process, it would give a more flexible approach. For this need are the wavelets good answer. [1, 2, 3]

2.3.3 Wavelet transform

Wavelet transform can be continuous or discrete. Continuous wavelet transform (CWT) of a function f is defined as

$$\hat{T}(a,b) = \frac{1}{\sqrt{a}} \int_{-\infty}^{+\infty} f(t)\psi(\frac{t-b}{a})\, dt, \tag{3}$$

where a is scale parameter, b is translation parameter and ψ is wavelet function.

In continuous wavelet transform the dilation and translation parameters a and b vary continuously. Restricting a and b to only discrete values of

$$a = a_0^m \tag{4}$$

$$b = nb_0a_0^m, \tag{5}$$

where m, $n \in Z$ and $a_0 > 1$ and $b_0 > 0$ are fixed, we get the discrete wavelet transform (DWT), which can be written as

$$\hat{T}_{m,n}(f) = a_0^{-m/2} \int f(t)\ \psi(a_0^{-m}t - nb_0)\, dt. \tag{6}$$

A family of wavelets is defined as

$$\psi^{a,b}(t) = \frac{1}{\sqrt{|a|}} \psi(\frac{t-b}{a}). \tag{7}$$

The function ψ is sometimes called “mother wavelet”, which is dilated or contracted by a and translated by b to generate a family of wavelets, $\psi^{a,b}$. Large values of the scaling parameter a mean large scale and they correspond to small frequency ranges, while small values of parameter a correspond to high frequencies and very fine scales. By changing parameter b wavelet function can be translated along the time axis: Each $\psi^{a,b}(t)$ is localized around $t = b$. An example of dilating and translating of Meyer wavelet is shown in figure 2.

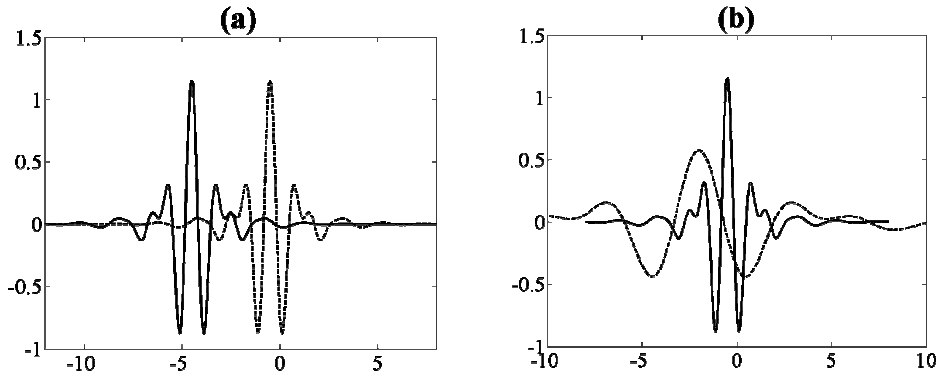

Figure 2. (a) Translation of Meyer wavelet with $b = 0$ (dash line) and $b = 4$ (solid line). (b) Dilation of Meyer function with $a = 1$ (solid line) and $a = 4$ (dash line).

Wavelet transform provides a time-frequency description of function f as did the windowed Fourier transform. A difference is in the shapes of the analyzing functions g and ψ. They are both shifted along the time axis but all the functions g have the same time-width while functions ψ have widths adapted to their frequency. At high frequencies $\psi^{a,b}$ are very narrow and at low frequencies they are much broader. This is why the wavelet transform gives a more flexible approach than windowed Fourier transform. With wavelet transform we can better zoom in on very short-lived high-frequency phenomena, like transients in signals or singularities in functions. Wavelets are mathematical microscopes that are able to magnify a given part of a function with a certain factor represented by a value of scale parameter. This magnification is associated with the extraction of the information at a certain scale hidden in a local area of the analyzed function.

In multiresolution analysis we need another function in addition to the analyzing wavelet, which is so called scaling function ϕ. A shifted and dilated (contracted) scale function is obtained as

$$\phi_{a,b}(x) = \frac{1}{\sqrt{a}}\phi(\frac{x-b}{a}). \tag{8}$$

Similar to wavelets, the scale parameter a and the translation parameter b can be expressed as $a = a_0^m$ and $b = nb_0a_0^m$ in the discrete scale function analysis. Usually the values $a_0 = 2$ and $b_0 = 1$ are used. The difference between wavelet and scaling function is that while wavelet function has zero mean

$$\int_{-\infty}^{+\infty} \psi(x)dx = 0, \tag{9}$$

the integral of scale function over the entire domain of x is unity

$$\int_{-\infty}^{+\infty} \phi(x)dx = 1. \tag{10}$$

Equation (10) stands for scale functions at $a = 1$, which are in most of analysis used. Equation (9) is valid for all scales and wavelets are usually used in higher resolutions.

An example of a wavelet with a scaling function is Meyer wavelet. The wavelet and the scaling function are represented in figure 3.

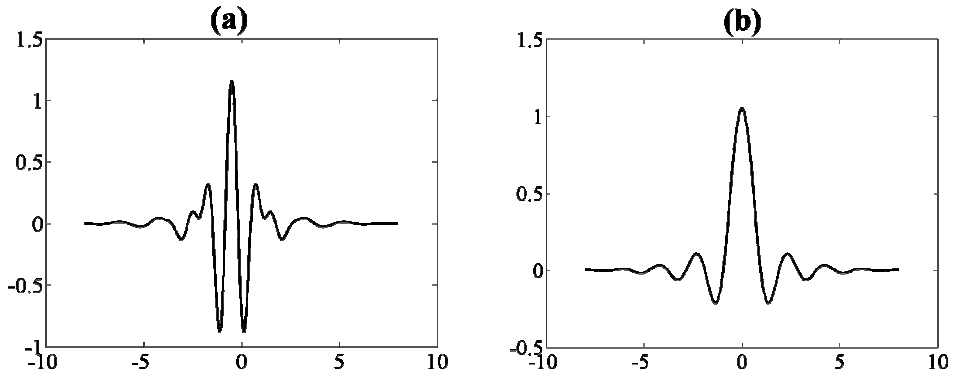

Figure 3. (a) Meyer wavelet and (b) Meyer scaling function.

It should be mentioned here that every wavelet does not have a scaling function. One such wavelet is the Mexican hat wavelet

$$\psi(x) = \left(\frac{2}{\sqrt{3}} \pi^{-\frac{1}{4}} \right) (1 - x^2) e^{-\frac{x^2}{2}} . \quad (11)$$

Wavelets with scaling functions are used in the analysis of functions with non-zero mean values. [1, 2, 3]

2.4 Features of wavelets

2.4.1 Admissibility and similarity

First demand for a function to be called a wavelet is admissibility. It means that the average of a wavelet, the analyzing function, should be zero (equation 9). Also all the functions of the wavelet family, obtained by translation and dilation of the "mother function", should be mutually similar. That means they have to be scale covariant with one another and should have a constant number of oscillations.

2.4.2 Regularity and invertibility

Wavelets should be sufficiently regular and they should be concentrated on some finite spatial domain. So they should be well localized on both sides of the Fourier transform. Another demand for wavelets is invertibility. It means that it should be possible to recover the original signal from its wavelet coefficients by a reconstruction formula.

2.4.3 Cancellations

Cancellations mean some vanishing high-order moments. This requirement is useful in some applications like turbulent signal analysis. It eliminates the most regular part of the signal and facilitates the study of high-order fluctuations and singularities in some high-order derivatives. [2, 3]

2.5 Choice of the wavelet and wavelet transform

Wavelets can be either real- or complex-valued functions. Most wavelets, for example Haar, Daubechies, Biorthogonal, Meyer, Gaussian, Marr (Mexican hat) and real Morlet wavelet are real-valued wavelets. However complex-valued wavelets have some advantages that real-valued wavelets do not have. Their phase shift between real and imaginary parts can prevent fake oscillations in wavelet transform coefficients and therefore they are preferred for transformation purposes.

In fluid mechanics and turbulence applications mostly used wavelet is the Complex Morlet wavelet

$$\psi(\frac{t-b}{a}) = \frac{1}{\pi^{1/4}} e^{\frac{-(t-b)^2}{2a^2}} e^{\frac{i\cdot 5(t-b)}{a}} . \qquad (12)$$

Figure 4 shows the real and imaginary parts of the Morlet wavelet.

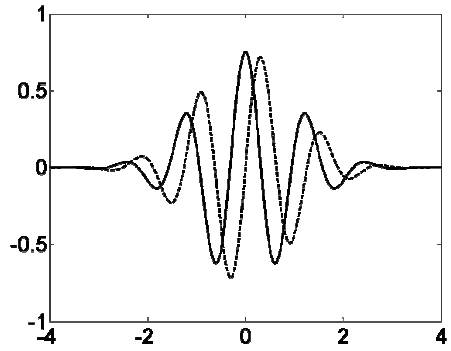

Figure 4. Morlet wavelet, solid line for real and dash line for imaginary part.

Other complex valued wavelets are complex-Gaussian, Shannon and mostly in quantum mechanics used Paul wavelet.

The qualities of wavelets vary according to several other criteria, such as symmetry, the number of vanishing moments, the regularity and the existence of scaling function. The symmetry of the wavelet is useful characteristic in avoiding dephasing

in image processing. The number of vanishing moments for wavelet or for scaling function is significant in compression purposes. The regularity of the wavelet has an effect on the smoothness of the reconstructed signal or image. For multiresolution analysis the best choice is a wavelet, which is associated with a scaling function, because the scaling function can see mean values, while the wavelets only see the fluctuations.

Wavelets and scaling functions are originally one-dimensional. For higher-dimensional problems we have to build a wavelet family using tensor products of wavelets and scaling functions. For instance two-dimensional scaling function and its associated wavelets can be defined as

$$\begin{cases} \phi(x,y) = \phi(x)\cdot\phi(y) \\ \psi_1(x,y) = \phi(x)\cdot\psi(y) \\ \psi_2(x,y) = \phi(y)\cdot\psi(x) \\ \psi_3(x,y) = \psi(x)\cdot\psi(y) \end{cases} \tag{13}$$

and in three dimensional case

$$\begin{cases} \phi(x,y,z) = \phi(x)\cdot\phi(y)\cdot\phi(z) \\ \psi_1(x,y,z) = \phi(x)\cdot\phi(y)\cdot\psi(z) \\ \psi_2(x,y,z) = \phi(x)\cdot\psi(y)\cdot\phi(z) \\ \psi_3(x,y,z) = \psi(x)\cdot\phi(y)\cdot\phi(z) \\ \psi_4(x,y,z) = \phi(x)\cdot\psi(y)\cdot\psi(z) \\ \psi_5(x,y,z) = \psi(x)\cdot\phi(y)\cdot\psi(z) \\ \psi_6(x,y,z) = \psi(x)\cdot\psi(y)\cdot\phi(z) \\ \psi_7(x,y,z) = \psi(x)\cdot\psi(y)\cdot\psi(z) \end{cases} \tag{14}$$

The choice of the transform depends on what kind of information we want to extract from the signal. The continuous wavelet transform is better suited for analysis of signals or fields, because due to its redundancy it shows the information content of the signal better than discrete wavelet transform. The discrete wavelet transform is a good tool for signal processing (denoising and compression) and for modeling

purposes, because of the orthogonality property and because it decomposes the signal into a minimal number of coefficients. [3]

3 TURBULENCE

3.1 General

Turbulence is fluctuating and disorderly motion. It consists of random pressure and velocity fluctuations and its nature is very complex. Most flows in nature and engineering applications are turbulent. Thus it is of interest in many fields of research: in dealing with atmospheric jet streams, in studying the photospheres of the sun, in calculating pipe flow, just to mention some.

Turbulent flows have been studied for more than a century and a lot is already known about turbulence and its structure, both physically and mathematically. However unpredictability and randomness of turbulence has made it difficult to fully understand, even with such powerful tools such as statistical mechanics. And the fact is that no completely formal theory of turbulence exists. This means that because of "non-deterministic" fluctuations in flow properties one cannot precisely predict the value of a flow property at a future instant by any known means, since the precise relationship is not known.

It has been observed that turbulent flows contain visible patterns, called coherent vortices, and a random part, the incoherent background flow. In standard analysis of turbulence it is common to divide the flow into two parts: time-averaged part and the fluctuation part.

There are two ways to handle turbulent flows: Statistical study of the properties of the fluctuations and semi-empirical modeling of turbulent mean quantities. The equations of motion have been analyzed in great detail, but statistical studies of the equations lead to a situation with more unknowns than equations. To reduce the number of degrees of freedom of the system of equations we can use a turbulence model in which the effects of the discarded modes on the retained modes are modeled. [2, 4, 5, 6, 7]

3.2 Properties of turbulence

When Reynolds number (*Re*) increases, laminar flow becomes unstable and turbulence occurs. The instabilities are related to the interaction of viscous terms and nonlinear inertia terms of the equations of motion. [5, 7]

Although turbulence is said to be irregular and disorderly motion, it has a spatial structure and the disorder is not only white noise. The organized structure can be characterized as eddies or fluid packets of many size. It is obvious that turbulent flows contain both an organized part, coherent vortices, and a random part, the incoherent background flow. These incoherent structures are associated with the Gaussian part of the flow, while organized patterns are responsible for the non-Gaussianity of the flow.

Coherent structures in turbulent flow contain most of the energy of the flow. Therefore the physics of turbulence can be related to the interactions between eddies of different sizes through a wide range of length scales from micrometer to meter. The role of large eddies is to transfer the kinetic energy to the smaller eddies while the smallest eddies dissipate the energy. [3, 4, 6]

Intermittency, which means the percentage of time the flow is turbulent, is an important property of turbulence. In an intermittent flow field rather calm periods are interrupted irregularly by strong turbulent bursts either in space or in time. Energy intermittency in turbulent flows is caused by the regeneration cycle of eddies. This self-sustaining characteristic is also a property of turbulent flow. It means that turbulence can maintain itself by producing new eddies to replace those lost by viscous dissipation. [6, 8, 9]

3.3 Modeling of turbulence

Computing turbulent flow is a challenge for scientific computing. Most of the turbulent flow theory is based on Navier-Stokes equations, which are derived from

the momentum equations. Navier-Stokes equations can be written in velocity vorticity formulation as

$$\partial_t \omega + \nabla(\omega \cdot V) - \nu \nabla^2 \omega = \nabla \times F \,, \tag{15}$$

where V is velocity field, ω is vorticity ($\omega = \nabla \times V$), ν is kinematic viscosity and F is external force. The difficulty in solving the Navier-Stokes equations is in the non-linear convection term $\nabla(\omega \cdot V)$. [4, 10]

3.3.1 Fully deterministic method

Fully deterministic simulations resolve all scales of motion and compute them deterministically. This is performed in direct numerical simulation (DNS). In DNS the number of degrees of freedom to be computed is highly dependent of the Reynolds number of the flow. The computation is limited to low Reynolds numbers and simple flow geometries because of the excessive amount of computing memory required. [4, 10]

3.3.2 Fully statistical models

It is possible to handle higher Reynolds number flows if we use a model to reduce the number of degrees of freedom to be computed. Only the steady mean flow is computed and the effect of the fluctuations on the mean is statistically modeled with a model based on measurements. The most popular method for computing turbulent flows is Reynolds Averaged Navier-Stokes (RANS) equations in which the flow field (e.g, velocity V) is split into mean $\overline{V}$ and fluctuations V', i.e. $V = \overline{V} + V'$. The mean value of the velocity can be computed as an ensemble average, time average or space average.

The averaging technique has a major role in modeling turbulence. If fluctuations whose effect is modeled have a Gaussian distribution, we can handle the non-linearity of the Navier-Stokes equations. However the classical averaging

techniques, which are used in RANS do not guarantee that the fluctuation part is really Gaussian. While computing the mean flow, RANS does not consider the spatial distribution of coherent vortices.

The standard k-ε model and Reynolds stress model are examples of RANS. Each of these models is related to a certain flow configuration and fitted parameters from laboratory measurements and they lack universality.

3.3.3 Semi-Deterministic methods

When some degrees of freedom are deterministically computed and the influence of the others is modeled, the method is said to be semi-deterministic. Large-Eddy Simulations (LES) and Unsteady Reynolds Averaged Navier-Stokes (URANS) equations belong to this category.

In URANS model the time evolution of the mean is computed, while in RANS model only a steady mean solution is computed. In LES the separation into computed modes and modeled modes is done by means of linear filtering between large scale and small scale modes. The small scales are assumed to be less important than the large scales. However it has been shown, that coherent vortices are multiscale. Thus LES using the Fourier low pass filter to eliminate the small scales, eliminates the small scales of the coherent vortices as well. So LES (and URANS) models can compute only a smoothed spatial distribution of coherent vortices.

Semi-deterministic methods are a good compromise of two aforementioned methods: they provide more physical insight than RANS and more realistic Reynolds numbers and more reasonable computational cost than DNS. However semi-deterministic methods can be improved by better characterizing the coherent structures, which are deterministically computed, and by controlling the Gaussianity of the discarded modes, whose effect on the retained modes is modeled.

One of these improved semi-deterministic methods is Coherent Vortex Simulation (CVS). It uses nonlinear wavelet filtering of the Navier-Stokes equations and is able to extract coherent vortices, without any smoothing. Background flow is then left free of organized structures and therefore their effect is easier to model. [4]

4 TURBULENCE AND WAVELETS

All classical methods to handle turbulence rely on the Fourier representation, and the dissipation term ($\nu \nabla^2 \omega$) of Navier-Stokes equation is optimally represented in Fourier space. However the non-linear convection term $\nabla(\omega \cdot V)$ is very complicated in Fourier space. When increasing the Reynolds number of the flow, non-linear term comes dominant and the Fourier representation is not any more adequate. To solve the non-linear convection term we need a more appropriate tool. [2, 11]

Tennekes and Lumley proposed, that turbulent flows could be thought as a superposition of Gaussian-shaped wave packets, eddies. Their description of an eddy (figure 5(a)) resembles greatly wavelets (figure 5(b)). Marie Farge was inspired by Tennekes and Lumley to introduce wavelet transform techiques to analyze, model and compute turbulent flows. [7, 11]

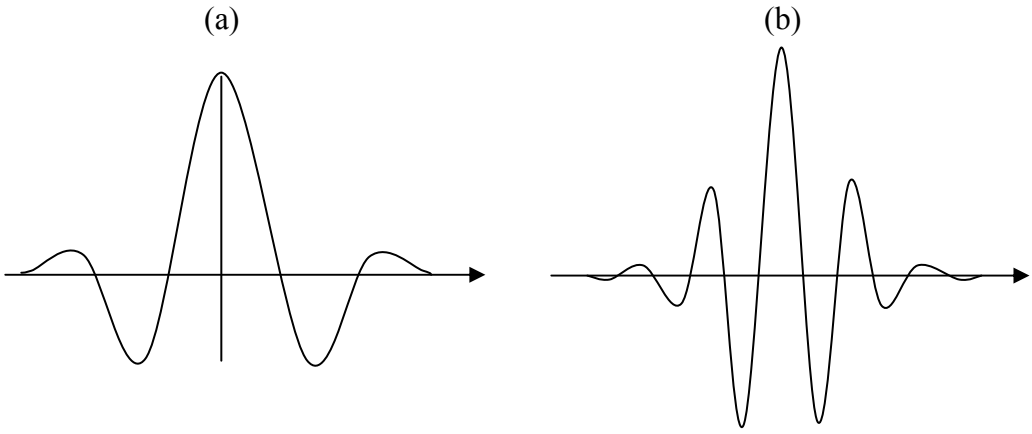

Figure 5. (a) An eddy, (b) real-valued Morlet wavelet.

4.1 Coherent vortex simulation

Coherent vortex simulation is a method, that uses wavelet decomposition to compute and model turbulent flows. Turbulent flow is separated into coherent and incoherent parts using the wavelet coefficients of the vorticity field. The evolution of the coherent vortices, which are localized consentrations of vorticity, is computed in a

wavelet basis. The incoherent components, which correspond to a homogenous random backround flow, are discarded while computing the flow evolution. The effect of the incoherent components on the coherent vortices is then modeled statistically.

4.1.1 Coherent vortex extraction

Extraction of coherent vortices in two-dimensional tubulent flow is done by developing the vorticity field $\omega(x,y) = \nabla \times V$ into an orthogonal wavelet series from the largest scale to the smallest scale. This is done using a two-dimensional multiresolution analysis (MRA). Vorticity field becomes

$$\omega(x,y) = \overline{\omega}_{0,0,0}\phi_{0,0,0}(x,y) + \sum_{j=0}^{J-1}\sum_{i_x}^{2^j-1}\sum_{i_y}^{2^j-1}\sum_{\mu=1}^{3}\widetilde{\omega}^{\mu}_{j,i_x,i_y}\psi^{\mu}_{j,i_x,i_y}(x,y), \qquad (16)$$

where ϕ and ψ are two-dimensional scaling functions and the corresponding wavelets respectively. The scaling coefficients, $\overline{\omega}_{0,0,0} = \langle \omega, \phi_{0,0,0} \rangle$, correspond to an approximation of $\omega(x,y)$ at the largest scale $j = 0$. The wavelet coefficients $\widetilde{\omega}^{\mu}_{j,i_x,i_y} = \langle \omega, \psi^{\mu}_{j,i_x,i_y} \rangle$ correspond to the details, that have to be added to approximate $\omega(x,y)$ from scale j to smaller scale $j + 1$. $\langle \cdot,\cdot \rangle$ denotes here an inner product.

The vorticity field ω is split into two components, coherent vorticity ω_C and incoherent vorticity ω_I, by applying a nonlinear thresholding to the wavelet coefficients. The threshold depends on the total enstrophy and the number of degrees of freedom. Coherent vorticity ω_C is then reconstructed from the wavelet coefficients whose modulus is larger than ε by inverse wavelet transform. The remaining weak wavelet coefficients are used to reconstruct the coherent vorticity ω_I.

The advantage of this method is that coherent vortices, that are extracted by retaining only 2% of the N wavelet modes, contain 99,01% of the total enstrophy, while the incoherent vorticity corresponds to 98% N modes and contains less than

1% of enstrophy. With CVS method it is then possible to reduce drastically the number of computed modes and to ensure the Gaussianity of the incoherent modes, whose effect is modeled. [4, 12]

4.1.2 Modeling the effect of the incoherent components

There are two ways to model the incoherent stress τ, which describes the effect of the discarded incoherent components on the retained coherent components. It can be treated as a weak forcing term, which reinjects a small percentage of the incoherent enstrophy lost by the CVS filtering. Other way to model the incoherent stress is to solve an linear advection-diffusion equation for the incoherent vorticity ω_I. [4]

4.1.3 Wavelet forcing

Wavelet forcing is a new way of forcing turbulent flows in numerical simulations. The role of forcing is to balance dissipation and obtain a statistically stationary state. Forcing is currently done in Fourier space, which means that the energy (in 3-D) and enstrophy (in 2-D) injected are not localized in physical space. When the forcing is performed in wavelet space, it is local in both space and scale. [4, 11]

4.1.4 Complex geometries

Complex geometries, such as walls, obstacles or containers of different shapes, in turbulent flows can be handled by adding penalization method to the CVS method. Solid walls or obstacles are modeled as a porous medium, which porosity η is tending to zero. The complex geometry is described by a masc function χ, which gets a value of 1 inside the solid region and 0 elsewhere. Navier-Stokes equations are then solved with an additional penalization term. [4]

4.2 Wavelets as a new diagnosis tool for signals

Continuous wavelet transform is a sophisticated tool for analyzing signals. It is like a mathematical microscope that enables the study of energy density distribution in

space-scale plane. One-dimensional signal is visualized in two dimensions, thus it makes possible to view the important features at various scales. Different patterns in continuous wavelet transform of a signal can be interpreted as the characters of the signal.

Figure 6 shows a signal, (a) that is a superposition of waves and (b) the energy density distribution of the signal (the modulus of the wavelet coefficients). The scale *a* is arbitrary in figures 6 and 7. Conelike pattern in the middle of the figure 6 (b) is caused by a sudden change in the signal. Conelike pattern can be seen in the wavelet transform when signal contains a local singularity (figure 6(c) and (d)). Conelike structure is pointing towards the point at the border of the half plane where the singularity is located. High regularity of the signal is reflected in the wavelet transform by a rapid decay of the coefficients.

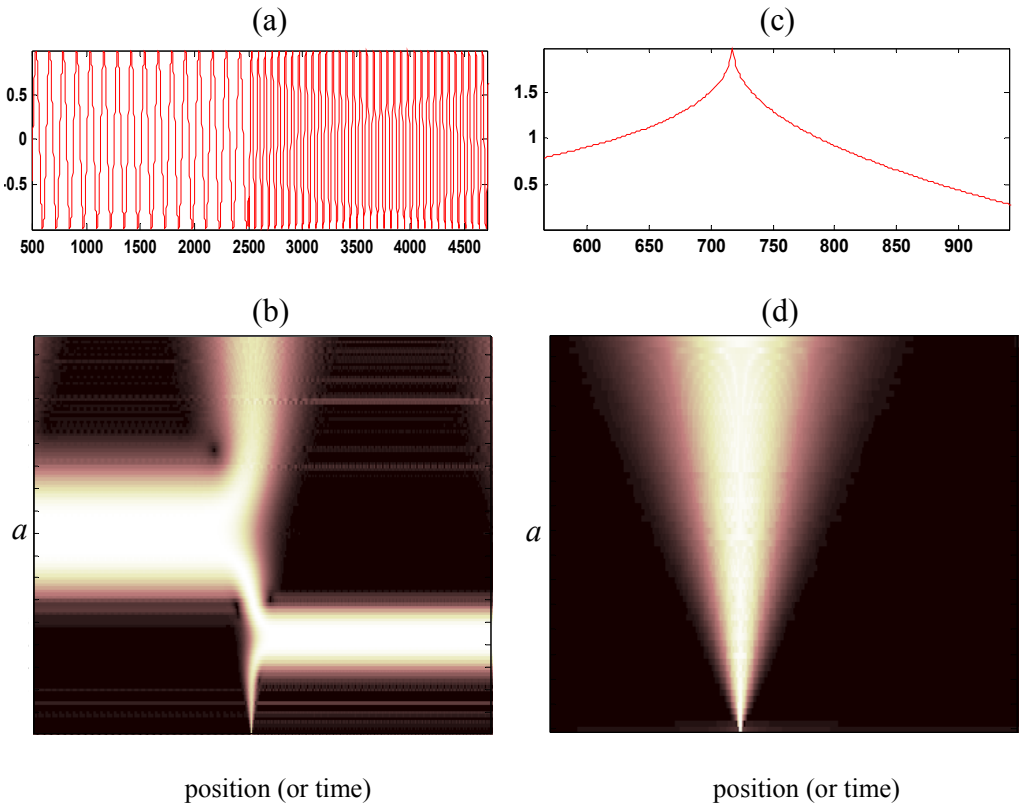

Figure 6. (a) Signal constructed of single frequencies, (b) wavelet transform of the signal (a), complex Morlet wavelet, (c) signal that is a set of localized structures, (d) wavelet transform of the signal (c), complex Morlet wavelet. Black and white colors represent minimum and maximum coefficients and other colors are interpolated.

Randomly distributed energy density like in figure 7 (a, b) describes Gaussian noise. In the figure 7 (c, d) we can see a repeating pattern that looks rougly the same on any scale. In that case the signal is called a self-similar signal.

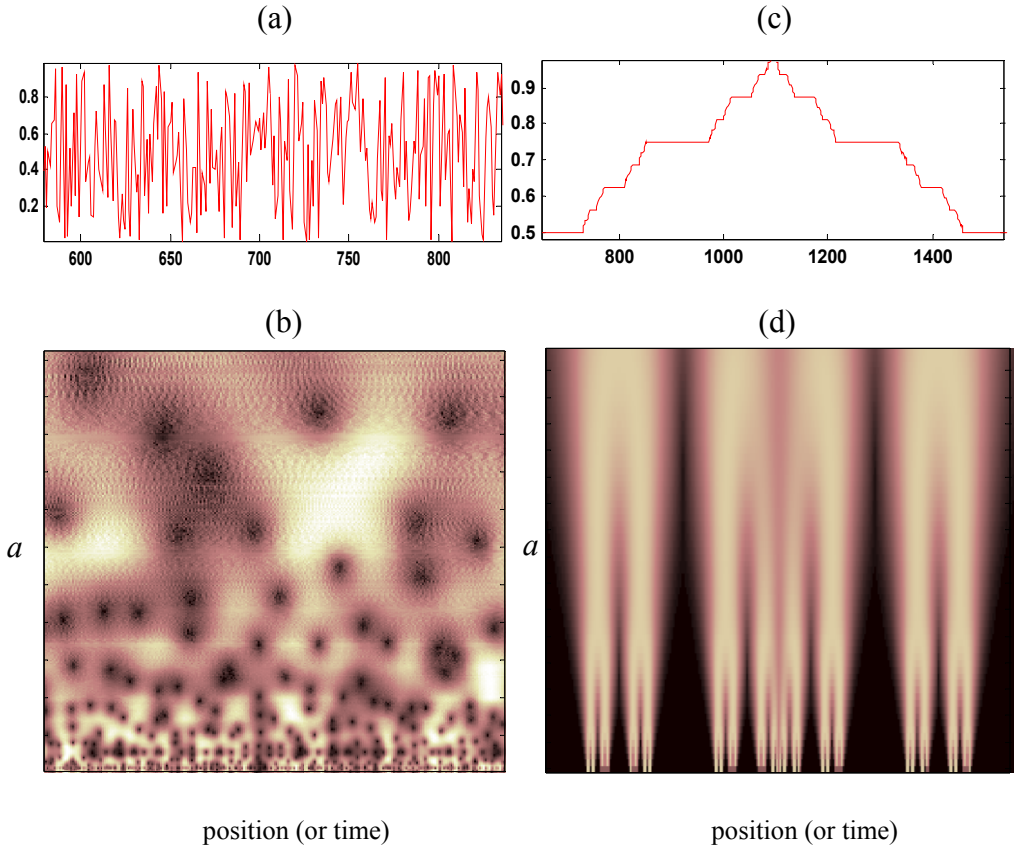

Figure 7. (a) Signal that is mainly noise, (b) wavelet transform of the signal (a), complex Morlet wavelet, (c) a self-similar signal (symmetric Cantor curve), (d) wavelet transform of the signal (c), complex Gaussian wavelet. Black and white colors represent minimum and maximum coefficients and other colors are interpolated.

When analyzing a signal or a field with wavelets, it is important to be aware of the fact that the continuous wavelet transform of a random signal can show correlation that is in the wavelet transform, but not in the signal itself. This can be checked with reproducing kernel, which is defined as

$$K_\psi(l_1, l_2, x_1, x_2) = C_\psi^{-1} \int_{-\infty}^{+\infty} \psi_{l_1 x_1} \psi^*{}_{l_2 x_2} dx \,. \tag{17}$$

Reproducing kernel can also be helpful in choosing the appropriate wavelet for a given problem.

Another danger in interpreting wavelet coefficients is to connect their strength with the strength of the signal while they really correspond to variations in the signal at a given scale and position. If there is no oscillation in the signal at a certain scale and position, the correspondig coefficients are zero. [2, 3]

5 WAVELET ANALYSIS FOR THE INTERMITTENCY IN TURBULENCE MODEL

Intermittency is an important characteristic of turbulence. The main goal of this work is to study the intermittency that a shell model of turbulence produces. The model studied here is the GOY shell model (Gledzer 1973, Ohkitani & Yamada 1989), which is a popular model for explaining turbulent intermittency. This intermittency is featured in the signal of energy dissipation rate through all related scales (wave numbers). The study will address two questions, the intensity of singular bursts, that interrupt the calm periods in an energy dissipation signal of the GOY shell model, and the frequency of occurrence for these singularities under certain conditions. Traditional Fourier transform analysis is unable to study each individual burst. The current analysis focuses on wavelets which are suitable for studying localized phenomena both in physical and scale (frequency) domains.

5.1 Shell model

5.1.1 Physical aspects

In turbulent flows, kinetic energy flows from large eddies to small eddies in a statistical sense. Eddies are characterized by a velocity scale u and a length scale l. The energy cascade is driven by vortex stretching and leads to viscous dissipation near the Kolmogorov's microscale. When a large eddy is in a strain-rate field, it undergoes stretching. The same happens with the smaller eddies that the large eddy contains. The plane strain field stretches the vortices as sketched in figure 8.

The equations for vorticity are

$$\omega_1 = \omega_0 e^{st} \qquad (\omega_1 > \omega_0) \tag{18}$$

$$\omega_2 = \omega_0 e^{-st} \qquad (\omega_1 > \omega_0) \tag{19}$$

$$\omega_1^{\,2} + \omega_2^{\,2} = 2\omega_0^{\,2} \cosh 2st\,, \tag{20}$$

where s is the strain-rate tensor, which is assumed to be constant for all $t > 0$, and $\omega_1 = \omega_2 = \omega_0$ at $t = 0$. Equation (20) shows that as t increases the amoumt of total enstrophy ($\omega_1^2 + \omega_2^2$) increases. Also, one can see that the energy exchange rate $T = s(u_2^2 - u_1^2)$ is positive during stretching. Therefore, the strain-field in a larger scale transfers kinetic energy to smaller scales.

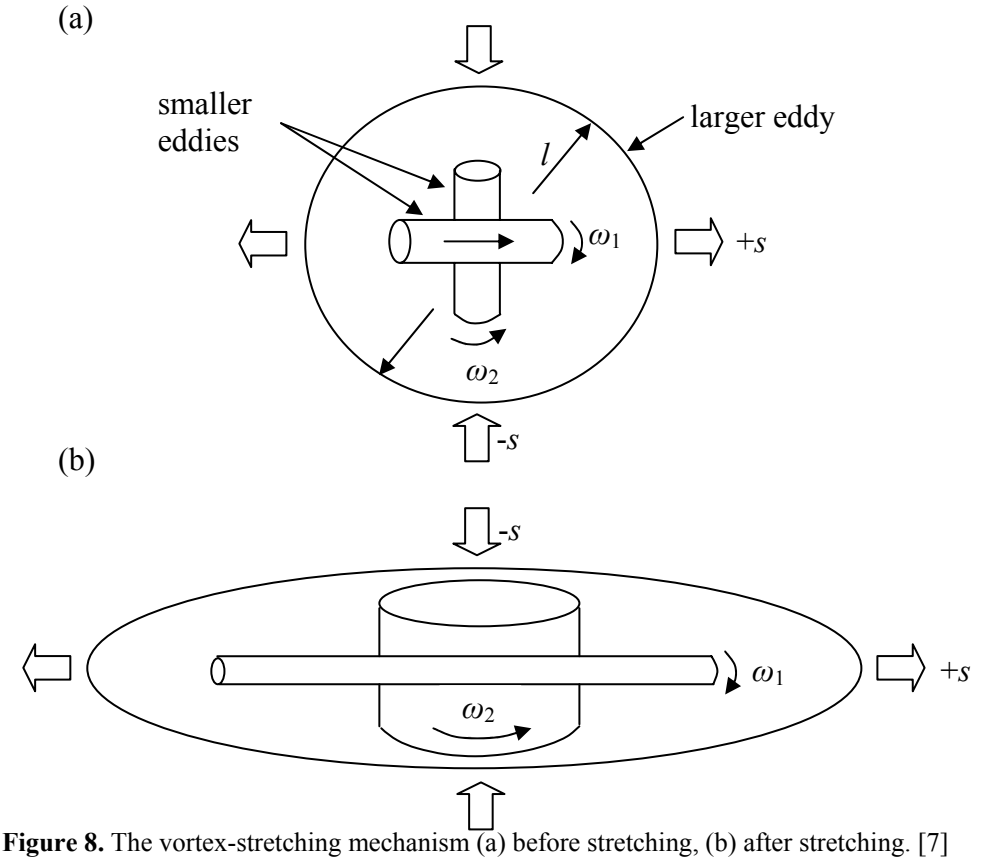

Figure 8. The vortex-stretching mechanism (a) before stretching, (b) after stretching. [7]

In Fourier space length l is represented by wave number k. If Navier Stokes equations are transferred to Fourier space, this wave number will replace the position. Wave number is a continuous variable and it is convenient to define some 'shells' that contain a spectrum of wave numbers. Navier Stokes equations are then expressed for each shell (in Fourier space) and the model is called a 'shell model'. [7]

5.1.2 Description of the model

Shell model is a class of cascade models, in which the energy transfer is assumed to be local in scale. From a statistical point of view, energy is injected at large scales and transferred from large scales to small scales and then dissipated into heat. In an instantaneous view of turbulence, a temporary energy flux can also be observed from smaller to larger scales, so-called backscattering, but the mean transfer is downscale. In cascade models turbulent field is characterized as a superposition of waves and the energy density is assumed to be distributed in phase space among horizontal bands, which correspond to excited wavenumbers. [9]

In shell models the governing equations (typically Navier-Stokes equations) are represented on a discrete set of wavenumbers in Fourier space. All Fourier modes with wave vectors $k_0 2^n < |k| < k_0 2^{n+1}$, are cast into a collective shell variable. Each shell is specified by a single wave number $k_n = k_0 2^n$, where n = 1,2,…,N. k_0 is a constant that represents the smallest wavenumber in the model and N is the total number of shells. The wave number k_0 is associated with the scale $L_0 = k_0^{-1}$ larger than which fluctuations do not exist. The velocity difference over a wavelength k_n^{-1} is described by the complex variable u_n. Alternatively, u_n can be thought as the velocity scale corresponding to the mean energy of the n-th wavenumber k_n.

The evolution equations in the GOY shell model are obtained according to four criteria: 1) The linear dissipation term is written as $-\nu k_n^2 u_n$. 2) The non-linear terms for u_n are given as quadratic combinations of the form $k_n u_{n'} u_{n''}$, n' and n" representing the nearest and next nearest neighbors of the n-th shell. 3) The interactions among shells are local in k-space and only the interactions between first and second-neighboring shells are considered. 4) The last criteria is the conservation of volume in phase space and the conservation of the total energy $\frac{1}{2}\sum_n |u_n|^2$, in absence of forcing and damping. With these criteria the evolution equations for the GOY model are as follows,

$$\frac{du_n}{dt} = -\nu k_n^2 u_n + f_n + ik_n (u_{n+1}^* u_{n+2}^* - \frac{1}{4} u_{n-1}^* u_{n+1}^* - \frac{1}{8} u_{n-1}^* u_{n-2}^*) , \qquad (21)$$

where f represents an external forcing term, active only in a few first shells, and superscript * means the complex conjugate. [8, 14, 15, 16]

An important advantage of using shell model is the possibility to reach large Reynolds numbers and reproduce the nonlinear dynamics of turbulence at a limited computational cost. In direct numerical simulations for three-dimensional turbulence the number of degrees of freedom is proportional to $Re^{9/4}$, whereas for shell models it only grows logarithmically in Reynolds. The weakness of the shell model is in loosing the information on geometry. The vectorial structure of the Navier-Stokes equations is lost and the details of the spatial structure of the flow are ignored. Shell models produce only temporal fluctuations in the cascade and ignore spatial intermittency, which is a character of real turbulence. In order to study both spatial and temporal fluctuations one would need to transform a chain model to a tree model. The spatial geometry can be achieved by multiplying the velocity field by a wavelet. The model describes the evolution of the wavelet coefficients of a one-dimensional projection of the velocity field. This tree model is not studied here. [16, 17]

Despite the lack of geometrical effects, the GOY model is rich in temporal and multiscale statistics that possesses many outstanding similarities with real turbulence. Better understanding of the intermittency of the GOY model can lead to an improved image of the intermittency in real turbulence. [2, 8, 11, 15, 18, 19, 20]

5.2 Results of the GOY model

The major parameters for the study of the GOY shell model have been chosen as follows. For the dimensionless kinematic viscosity, cases with $\nu = 10^{-4}$, $\nu = 10^{-5}$, $\nu = 10^{-6}$ and $\nu = 10^{-7}$ have been considered. The resulting Reynolds number is in the order of $Re \sim \nu^{-1}$. Parameters f_0 and k_0 have been set to 1 for all the main cases.

Information for simulated cases is given in table 1. Hereafter, we make the following convention to name different simulated cases. The name starts with "R" followed by the case category given in table 1. The second part of the name starts with "N" followed by the number of shells. For example, R1N12 represents the case with $Re \sim 10^4$ using 12 shells. In addition a few cases have been run using different values of f_0 to investigate the effects of external forcing. Results are presented for variation of u_n, dissipation of each shell and the overall dissipation.

Table 1. Basic parameters for studied cases.

Case category	Reynolds number (Re)	Shell numbers (N)
1	$\sim 10^4$	10, 11, .. , 15
2	$\sim 10^5$	10, 11, .. , 16
3	$\sim 10^6$	10, 11, .. , 18
4	$\sim 10^7$	10, 11, .. , 21

Note that all variables and parameters are dimensionless in this model.

5.2.1 Variation of characteristic velocities of shells (u_n)

To view the general behavior of the model, variation of $|u_n|$ versus time is shown in Fig. 9 for different values of Re as well as the time evolution of the total energy dissipation. In order to reduce overlapping, u_n time series have been shifted down by the value of $n/4$. The figures show that the fastest variations in u_n happen in higher wave numbers (small-scale shells) whereas very slow variations of u_n occur within lower wave numbers (large-scale shells). Also the absolute values of u_n are smaller in higher wave numbers. Other feature that stands out from the figures is how the disturbance in u_n time series moves among the shells starting from the lower wave numbers spreading into the higher ones via a chain reaction. [20]

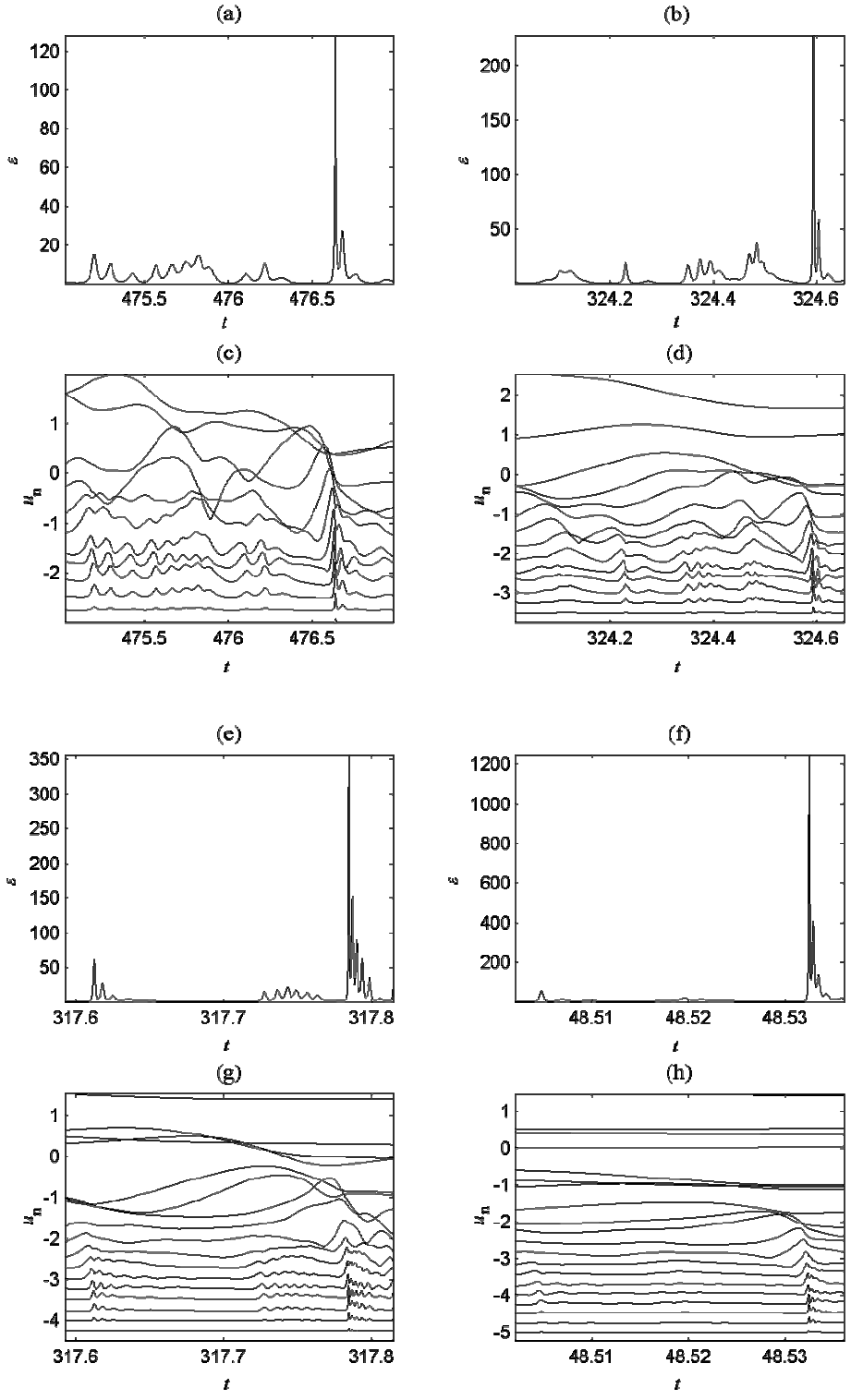

Figure 9. Time evolution of energy dissipation rate for cases (a) R1N12, (b) R2N15, (e) R3N18, (f) R4N21 and absolute values of u_n for the corresponding cases (c) R1N12, (d) R2N15, (g) R3N18, (h) R4N21. The u_n-time series (n = 1, 2,.., N) have been shifted down by the value n/4. The shell number n grows downwards.

5.2.2 Energy dissipation rate

The energy dissipation is an important quantity demonstrating intermittency in time and space. In the GOY shell model we only have time intermittency as spatial information are absent. The overall dissipation rate is defined as a summation of dissipation rates at different shells as follows:

$$\varepsilon(t) = \nu \sum_{n=1}^{N} k_n^2 \left| u_n(t) \right|^2 . \tag{22}$$

The time evolution of energy dissipation for different *Re* can be observed through figures 10(a)-(d). The insets of the figures show the propability density function (PDF) of each case. The slope of the PDF characterizes the intermittency of the signal. Sharper slope refers to a lower propability of finding large fluctuations in the dissipation signal. The values of the slopes in figure 10 are presented in table 2. One can see that the propability of finding large fluctuations in the signal is higher for larger values of Reynolds numbers, i.e. the larger the Reynolds number the larger the degree of intermittency. [2, 8]

Table 2. The values of slopes in insets of figure 10.

Case	Slope
R1N12	-3.2
R2N15	-3.1
R3N17	-2.7
R4N19	-2.2

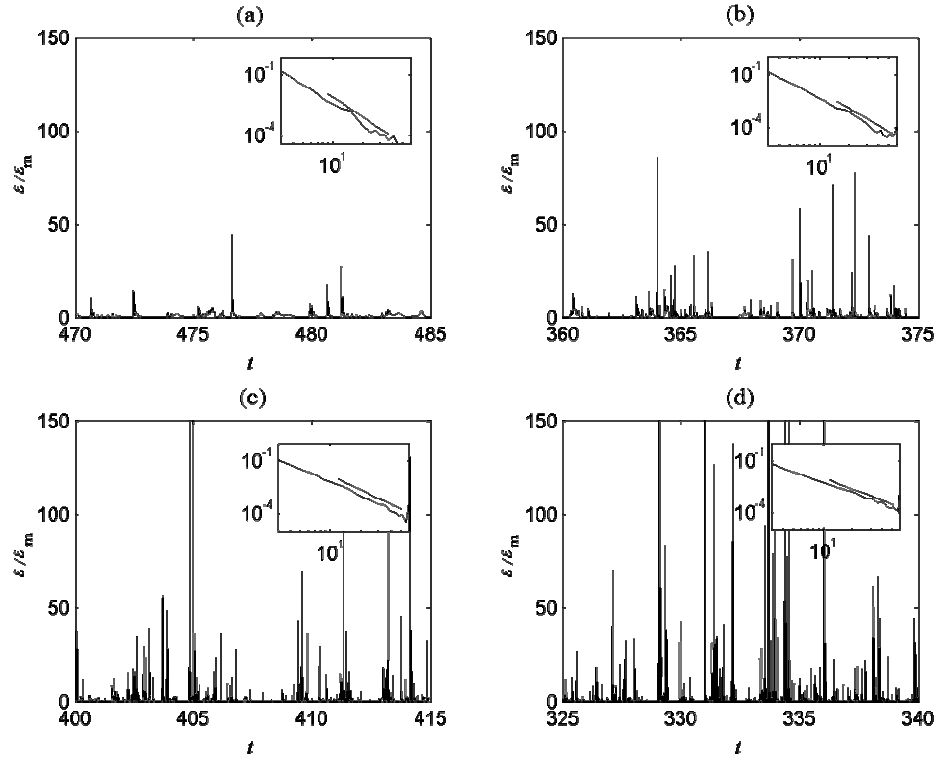

Figure 10. Time evolution of energy dissipation rate for cases (a) R1N12, (b) R2N15, (c) R3N17, (d) R4N19. The values of dissipation are normalized by their mean values. Insets: Probability distribution functions (PDF) of the corresponding cases.

Figures 11(a)-(h) represent the energy dissipation at different shells for a variety of Reynolds numbers at a certain forcing (f_0 = 1). It can be seen that the first shells (larger scales) do not dissipate the energy at all. It can also be observed that in a certain *Re* the number of active shells N_a remains constant. Further increase in shell numbers will not affect the results including total dissipation. This means that for the shells $n > N_a$, corresponding dissipation ε_n of the shell will remain zero.

In the next section the energy dissipation bursts produced by the GOY shell model will be studied. Wavelets, which can be seen as a mathematical microscope, suit well for the analysis of singularities because of their localized properties in both space (time) and scale.

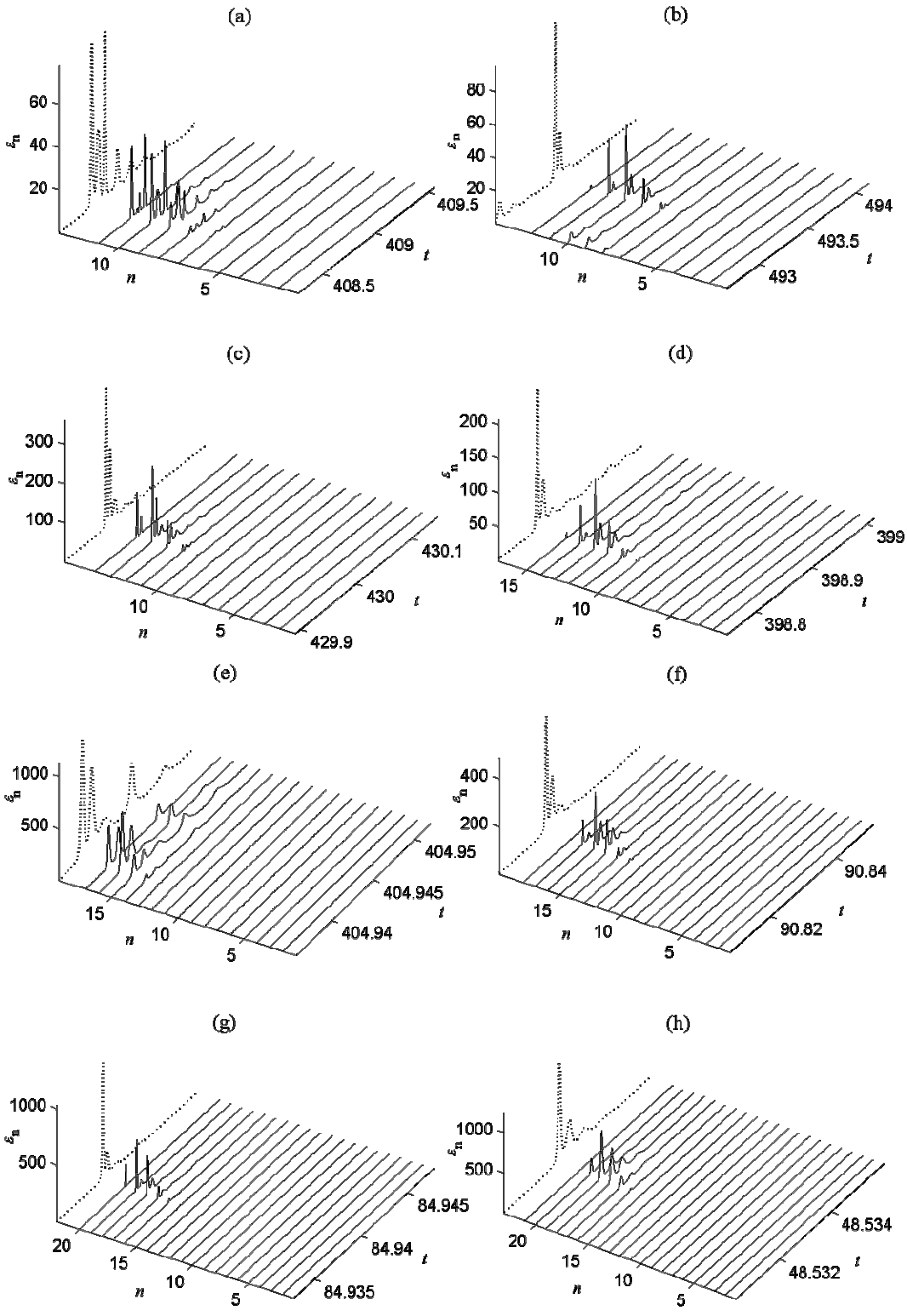

Figure 11. Time evolution of energy dissipation of each shell number n (solid line) and the total energy dissipation (dotted line) for cases: (a) R1N11, (b) R1N12, (c) R2N14, (d) R2N15, (e) R3N17, (f) R3N18, (g) R4N20, (h) R4N21.

5.2.3 Effect of external forcing

Figure 12 shows the variation in the amplitude of mean energy dissipation when the external forcing term f_0 is increased from one to ten.

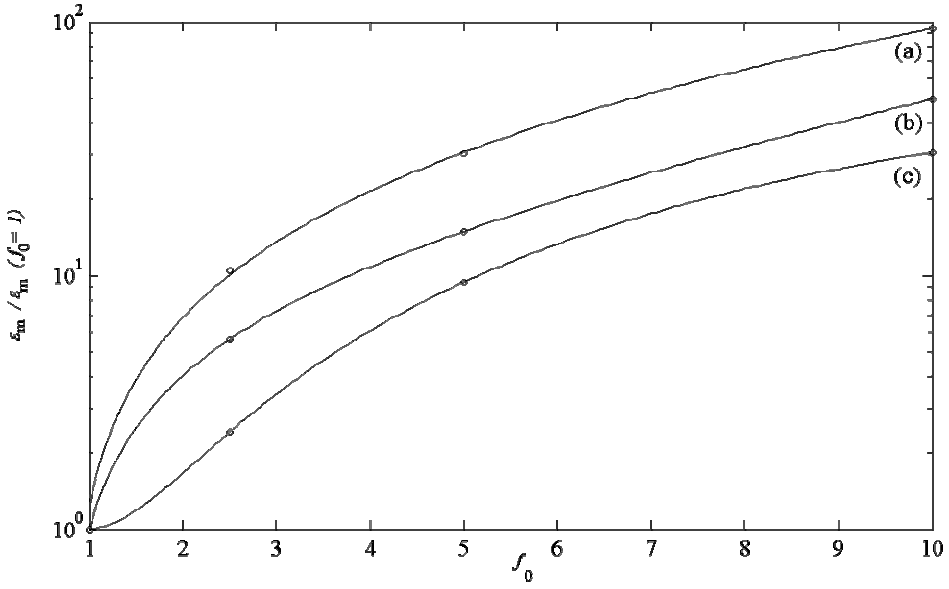

Figure 12. The change in the mean energy dissipation when external force is 1, 2.5, 5 and 10 for cases (a) R2N15, (b) R3N18, (c) R4N21. The values of dissipation are normalized by the value of mean dissipation at $f_0 = 1$.

In this figure polynomials represent variation of normalized dissipation rate versus f_0. As forcing term increases dissipation rate increases sharper for lower Reynolds numbers. For instance, when f_0 is increased from 1 to 10 the dissipation rate is amplified by a factor of 500 for $Re \sim 10^4$, 100 for $Re \sim 10^5$, 50 for $Re \sim 10^6$ and 30 for $Re \sim 10^7$.

5.3 Wavelet analysis of the intermittency in the GOY model

In the previous section it was shown that the dissipation signal of the shell model is intermittent and that the intermittency varies with Reynolds number. Intermittency means localized bursts of high frequency activities, therefore, it is a phenomenon that is local in both physical and spectral space. An interesting question is whether the quality of the singular bursts is different for different cases that were introduced

in the previous section. Also the frequency of occurrence for the dissipation peaks in the signal will be studied.

First the power spectral density of dissipation signals will be shown, which demonstrate the energy spectra of the signals. The Fourier basis is well localized in spectral space but totally delocalized in physical space and can not therefore give any information of individual singularities. Another tool is needed in order to study the character of the singular bursts in the signal. That tool is continuous wavelet transform.

To measure the intermittency of the dissipation signal the space-scale information contained in the wavelet coefficients of the continuous wavelet transform is utilized. The localization property of wavelets in the domain of scale is the answer to the question of intensity of the singular bursts and the localization property in time (space) can represent the frequency of occurrence for the bursts in the signal. Two measures, the local scaling exponent α and the partition function Z, will be introduced in the following subsections for that purpose. The cases that will be studied here for intermittency have been chosen consistent to the previous section. Reynolds numbers for the cases are $Re \sim 10^4$, 10^5, 10^6, 10^7. Shell numbers for each Reynolds number have been chosen as described in section 5.2.2 (figure 11).

5.3.1 Fourier transform

The frequency content of a signal can be analyzed with power spectral density (PSD). It describes the distribution (over frequency) of the power contained in a signal and it is mathematically related to the correlation sequence by the discrete-time Fourier transform. PSD is given as power per unit of frequency.

Figure 13 shows the power spectral density of dissipation rate signals of studied cases. From the figure it can be seen that the power per unit of frequency increases when Reynolds number and shell number are increased. However, PSD fails to reveal the information of individual bursts occurring in the original signal. This

leads us to implement continuous wavelet transform to study any single burst existing in a signal.

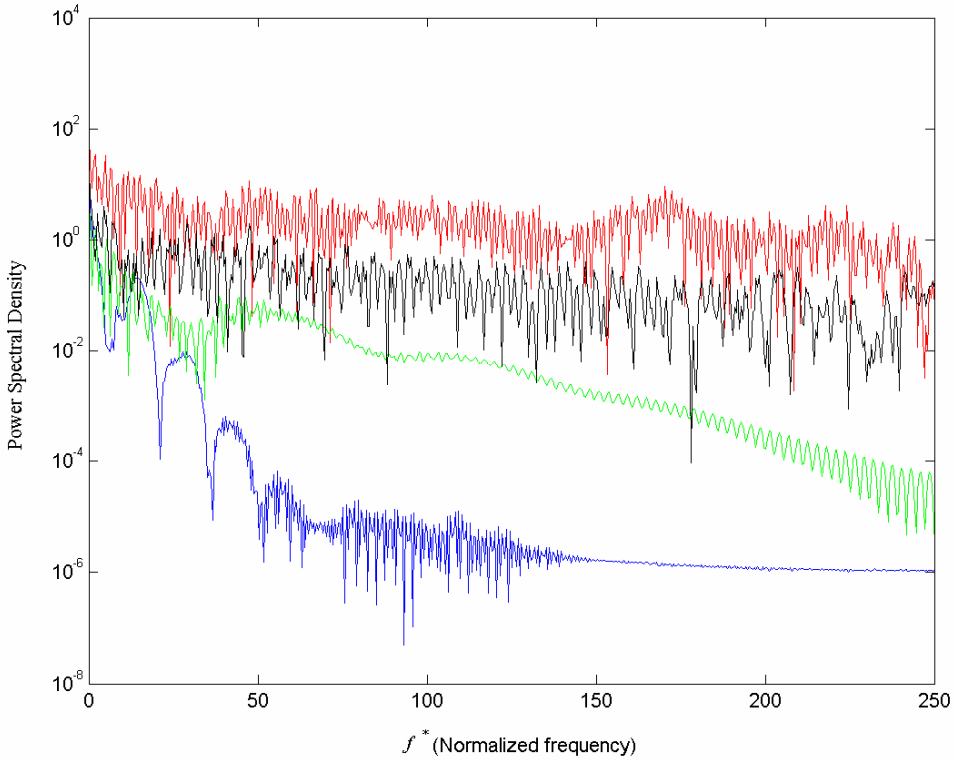

Figure 13. Power spectral density (PSD) of the dissipation rate for cases R1N12 (blue), R2N15 (green), R3N18 (black) and R4N21 (red).

5.3.2 Continuous wavelet transform

Wavelet toolbox of MATLAB is used to perform the continuous wavelet transform on dissipation signals of different cases. The wavelet used here is complex Morlet wavelet. First of all the dynamics of the dissipation signal is studied to realize how it is affected by the number of shells *N*. The plots of the modulus of the wavelet coefficients in time-scale plane (figures 14(a)-(d)) show how the behaviour of the signal changes, when the number of shells is increased. If the number of shells is too low, the behaviour of the dissipation signal is periodic and not intermittent. If the number of shells is increased the behaviour will gain randomness and finally intermittent. When *N* is increased even more, the periodic behaviour will vanish and

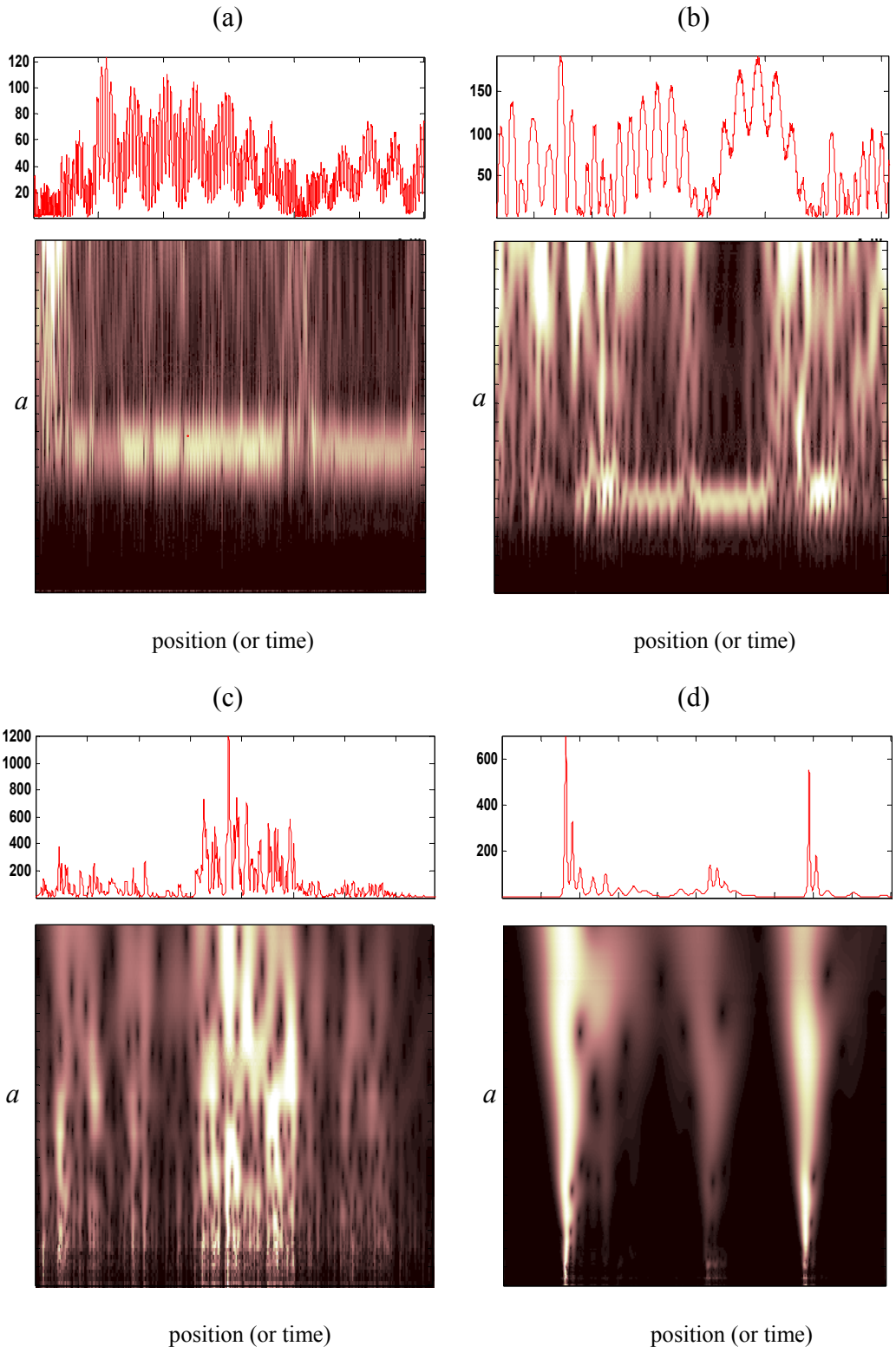

Figure 14. Dissipation rate and its wavelet transform of cases (a) R4N11 (periodic behaviour) (b) R4N12 (periodic and random), (c) R4N17 (intermittent and random), (d) R4N20 (intermittent and random). Complex Morlet wavelet. Black and white colors represent minimum and maximum coefficients and other colors are interpolated.

signal will be only random and intermittent, which is characteristic of real turbulence.

5.3.3 Strength of the singularities

A very useful property of the wavelet transform is its ability to measure the strength of individual singularities in a given signal. A local singularity in a signal produces a conelike structure in the wavelet transform pointing towards the point x_0, where this singularity is located. The position x_0 of a singularity can be found by following the position of a wavelet modulus maximum of the wavelet transform $|\hat{T}(x,a)|$ as the scale $a \to 0^+$. The wavelet transform modulus for the singularity satisfies

$$\left|\hat{T}(x_0,a)\right| \le Aa^{\alpha(x_0)}, \tag{23}$$

in the limit $a \to 0^+$. $\alpha(x_0)$ is the local scaling exponent that describes the strength of the singularity located at x_0. The exponent α is determined by the slope of $\ln|\hat{T}(x_0,a)|$ plotted versus $\ln a$. [11, 12, 13, 21, 22, 23]

Figure 15(a) shows one dissipation peak in a dissipation signal, (b) its wavelet transform and inset the curve of WT modulus maxima. The modulus maxima shows the beginning of the singularity in the small scales and the center of the dissipation peak at larger scales. Therefore, two different scaling exponents will be considered for each singularity, namely the small-scale exponent α_s for lower range of scales, and the large-scale exponent α_l for higher range of scales.

(a)

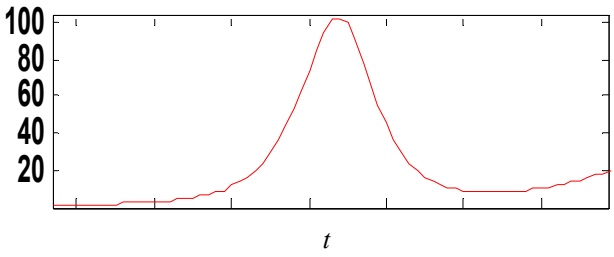

(b)

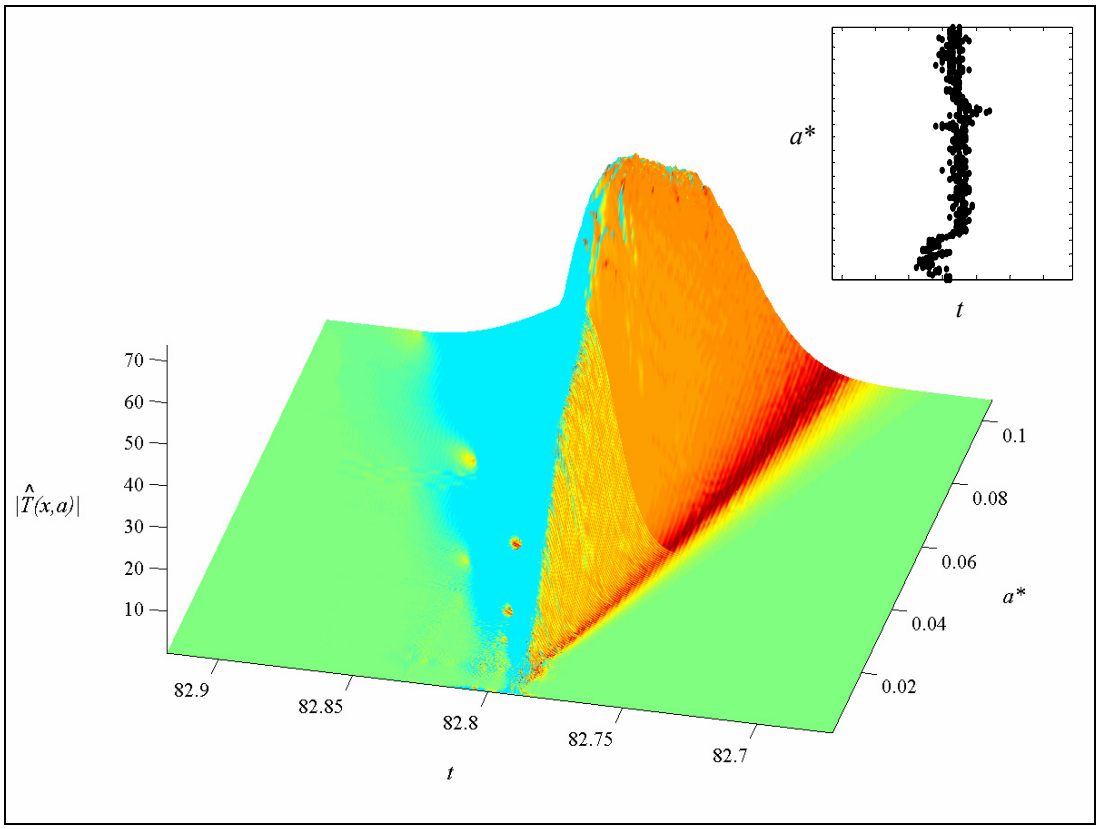

Figure 15. (a) One dissipation peak in a dissipation signal of case R2N15, (b) its wavelet transform. Complex Morlet wavelet. Inset: The curve of WT modulus maxima.

The cases for study have been chosen according to the criteria presented in section 5.2.2 (figure 11). The critical number of shells for each Reynolds number is shown in figure 16(a). The cases to be studied are thus R1N12, R2N15, R3N18, R4N21. In each case several dissipation peaks are studied using wavelet transform.

As described earlier, $\ln|\hat{T}(x_0, a)|$ is plotted versus ln$a$ and the slopes α_s and α_l are determined. Figure 17 shows an example of determining the slopes. The scale parameter (given by MATLAB's wavelet toolbox) has been normalized using a reference value introduced below. Different signals have different sampling times Δt and therefore different number of data points in the unit of time. In order to compare different signals with various sampling rates a global scale is needed, which is independent of the sampling rate..

The scales are determined in MATLAB according to the number of data points N_d as

$$\frac{N_d}{2} \geq 2^{\beta}, \tag{24}$$

where 2^{β} is maximum scale a_{max} and β is an integer number. The number of data points in signal in the unit of time is $N_{d,0} = 1/\Delta t$ and the corresponding scale is $a_0 = 2^{\beta_0}$. β_0 is derived from equation (24) as being an integer number

$$\beta_0 = [\log_2 N_{d,0} - 1]. \tag{25}$$

Here, the brackets [.] results the integer part of its argument. Global scale a^* can then be calculated by dividing the scale a (given by MATLAB) by the scale a_0.

The mean values of the slopes for each studied case have been calculated from several dissipation peaks. The mean values of the slopes are presented in table 3, and figure 16(b) shows the slopes with deviation for different cases.

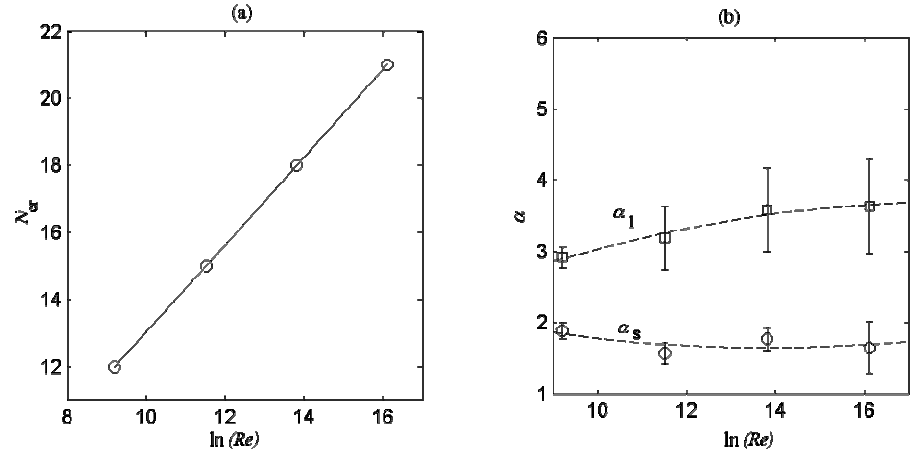

Figure 16. (a) The critical number of shells for different Reynolds numbers, (b) the mean values of the small-scale exponents α_s (circles) and the large-scale exponents α_l (squares) for different Reynolds numbers with critical number of shells. Deviation is shown for each case.

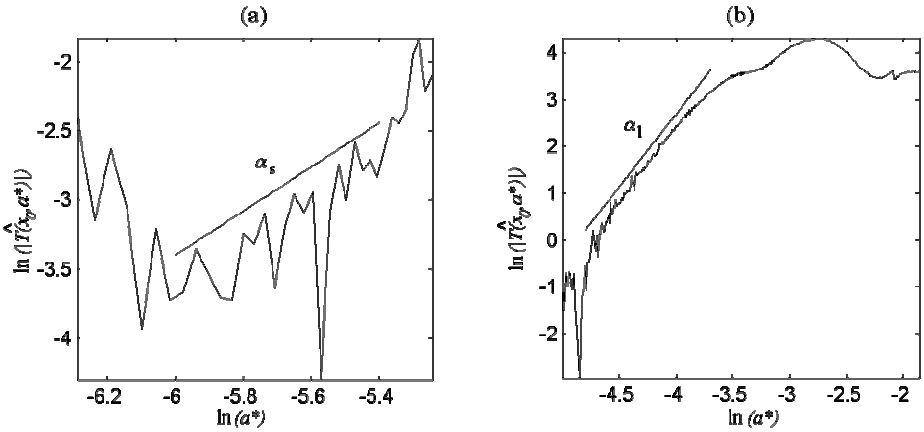

Figure 17. ln-ln plot of the WT amplitude versus the normalized scale a^* of one dissipation peak of case R2N15: (a) The prestage slope α_s, (b) the developed stage slope α_l.

Table 3. The mean values of the slopes of dissipation peaks.

Case	Small-scale exponent (α_s)	Large-scale exponent (α_s)
R1N12	1.88	2.93
R2N15	1.57	3.18
R3N18	1.77	3.58
R4N21	1.65	3.63

As the Reynolds number increases, the large-scale exponent slightly increases while the small-scale exponent remains quite the same. Larger values of α mean more local singularities. Also one can see from figures 18(a)-(d) that as the Reynolds number increases the range of corresponding global scales shifts to smaller scales. It means that at high Reynolds numbers (~10^7) singular bursts are measured by scales several orders of magnitude smaller than low Reynolds number (~10^4).

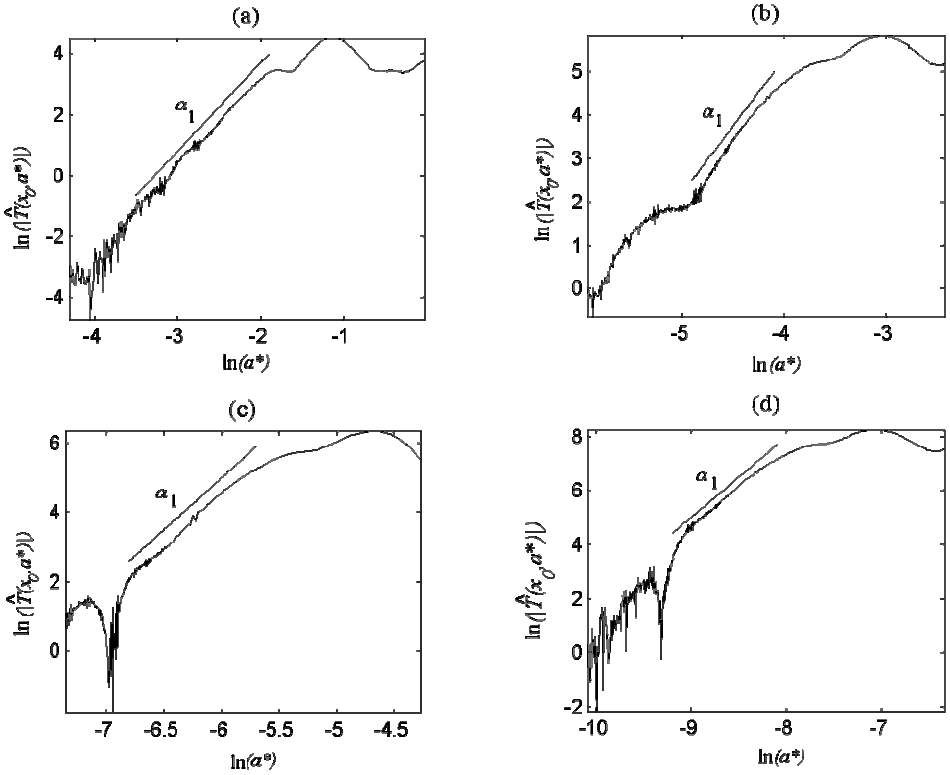

Figure 18. log-log plot of the WT modulus at the center of the dissipation peak versus scale a for cases (a) R1N12, (b) R2N15, (c) R3N18 and (d) R4N21.

The character of the singularities also changes if the shell number N is too low or too high. Figure 19 shows how the slope α_1 moves from larger scales to smaller scales as the shell number is increased and thus the singularities gain small scale behaviour. Also the value of the exponent increases when increasing the shell number and singularities become more local.

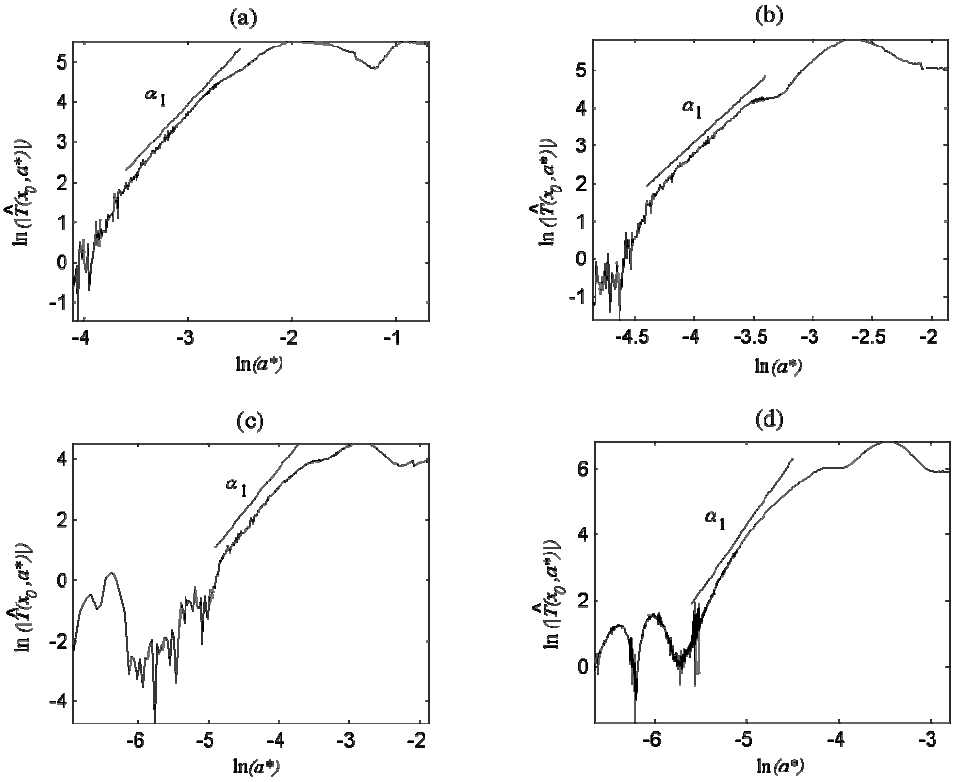

Figure 19. log-log plot of the WT amplitude of the central of the dissipation peak versus the scale *a* for cases (a) R2N13, (b) R2N14, (c) R2N15 and (d) R2N16.

5.3.4 Partition function

A method for computing the singularity spectrum of a signal is to define a partition function *Z* taking advantage of the space-scale partitioning given by the maxima representation of the wavelet coefficients. Partition function is defined as

$$Z(a,q) = \sum_{\{x_i(a)\}_i} \left|\hat{T}(a,x_i(a))\right|^q \sim a^{\tau_q} . \tag{26}$$

The wavelet coefficients are not summed over the whole set of wavelet coefficients but only over the WT modulus maxima $\{x_i(a)\}_i$ at a given scale *a*. The partition function scaling exponent τ_q represents the singularity spectrum of the signal. [11, 23, 24]

Figure 20 shows the partition function of different cases with different values of q.

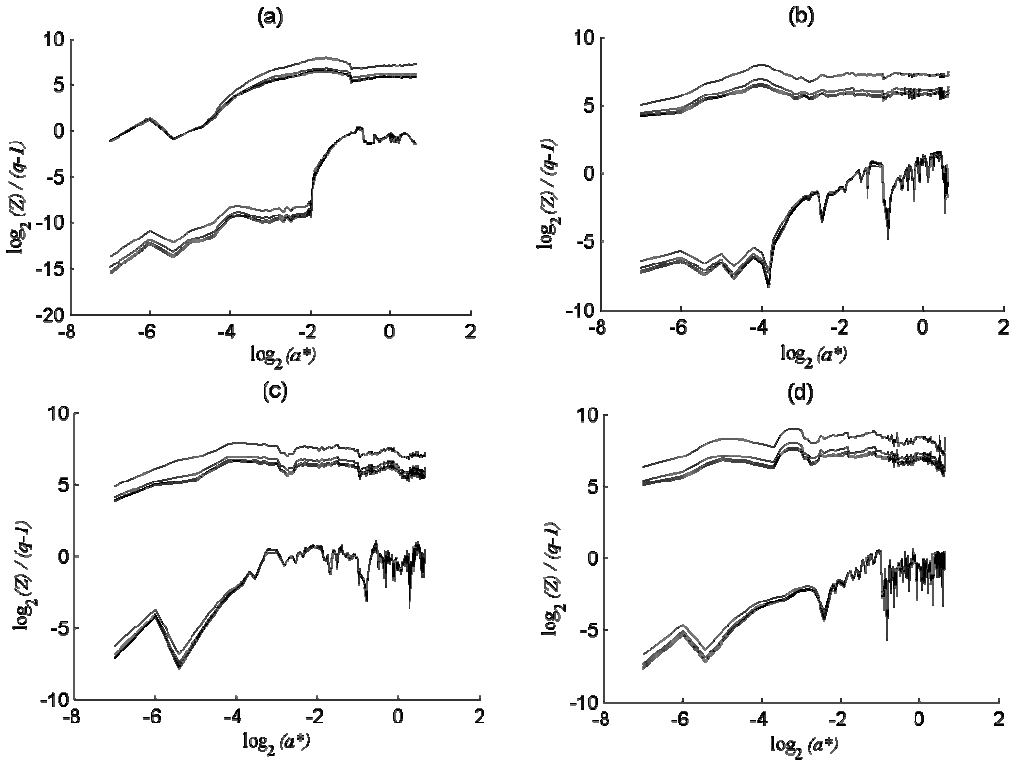

Figure 20. $\log_2(Z(a,q))/(q\text{-}1)$ vs $\log_2(a^*)$ for cases (a) R1N12, (b) R2N15, (c) R3N18 and (d) R4N21. Values of q from up to down in each figure: 5, 10, 15, 20, -5, -10, -15, -20.

To compare the intermittency of studied cases the values of q were determined, by which the intermittency of each case should be scaled to mach the intermittency of the others. Figures 21 and 22 show an example of scaling of cases R2N15, R3N18, R4N21 and R1N12. The case R1N12 have a different behavior than others so that its corresponding partition functions could be scaled with other cases either within small scales or within large scales. Therefore different scaling factors q will be presented in lower and higher scales for the case R1N12.

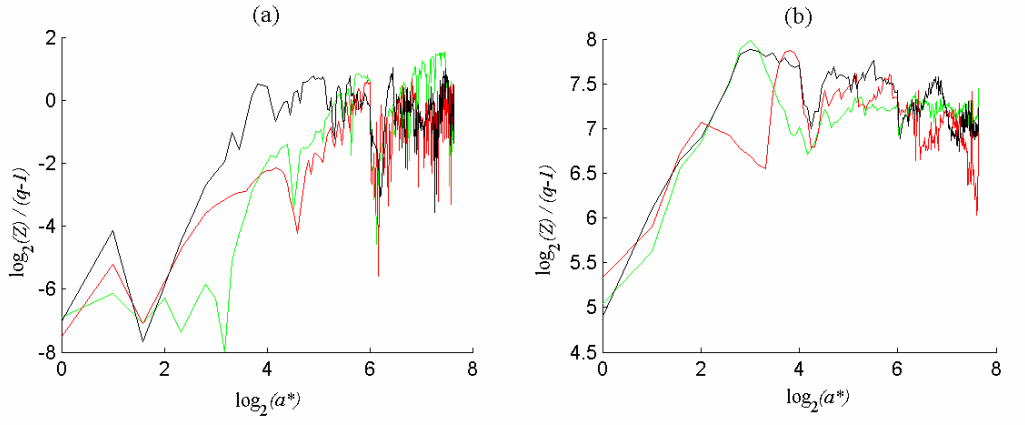

Figure 21. The scaling of cases R2N15 (green), R3N18 (black) and R4N21 (red). Values of q in figures: (a) R2N15: q = -10, R3N18: q = -15, R4N21: q = -15 (b) R2N15: q = 5, R3N18: q = 5, R4N21: q = 12.

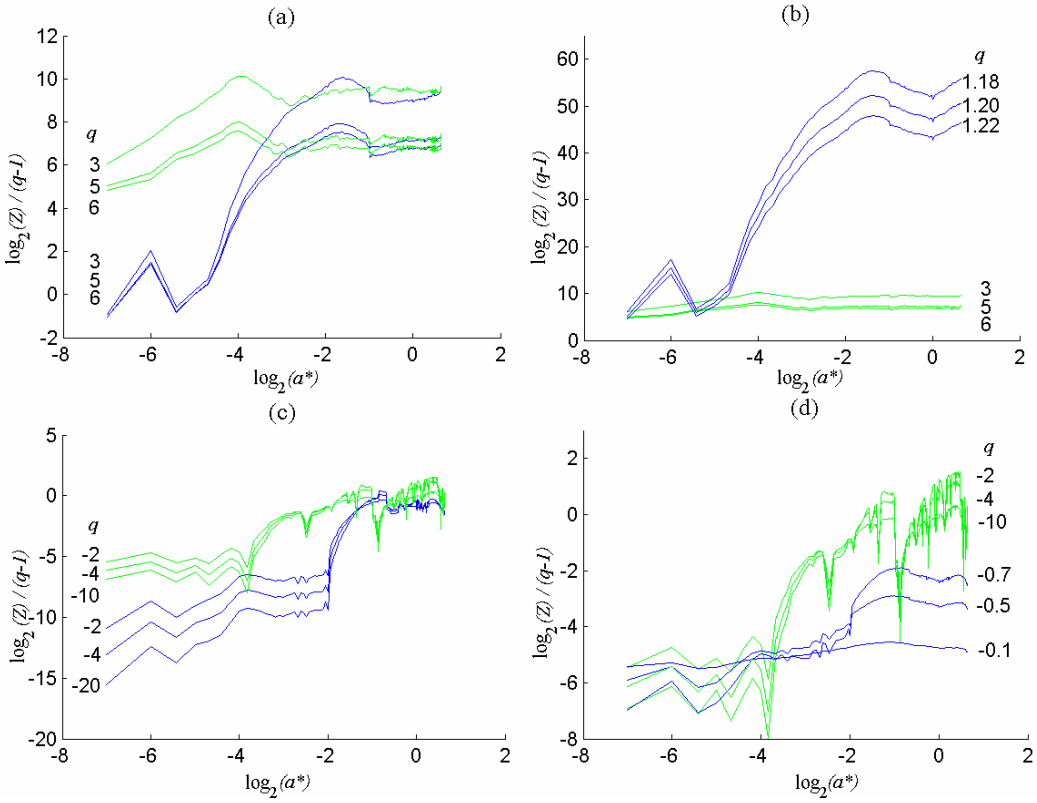

Figure 22. The scaling of case R2N12 (blue) with case R2N15 (green).

The values of scaling factor q are presented in table 4. The values of q for cases R2N15, R3N18 and R4N21 are also presented in figure 23 showing the scaling of

different cases. The figure reveals that the intermittency of cases R2N15 and R3N18 is approximately at the same level and the intermittency of case R4N21 is higher.

Table 4. The values of q to scale the intermittency.

Case	q						
R1N12 small scales	- 0.7	- 0.5	- 0.2	- 0.1	1.18	1.20	1.22
R1N12 large scales	- 20	-7	-4	-1	3	5	6
R2N15	-10	-7	-4	-1	3	5	6
R3N18	-15	-9	-5	-2	3	5	7
R4N21	-15	-10	-5	-2	4	12	24

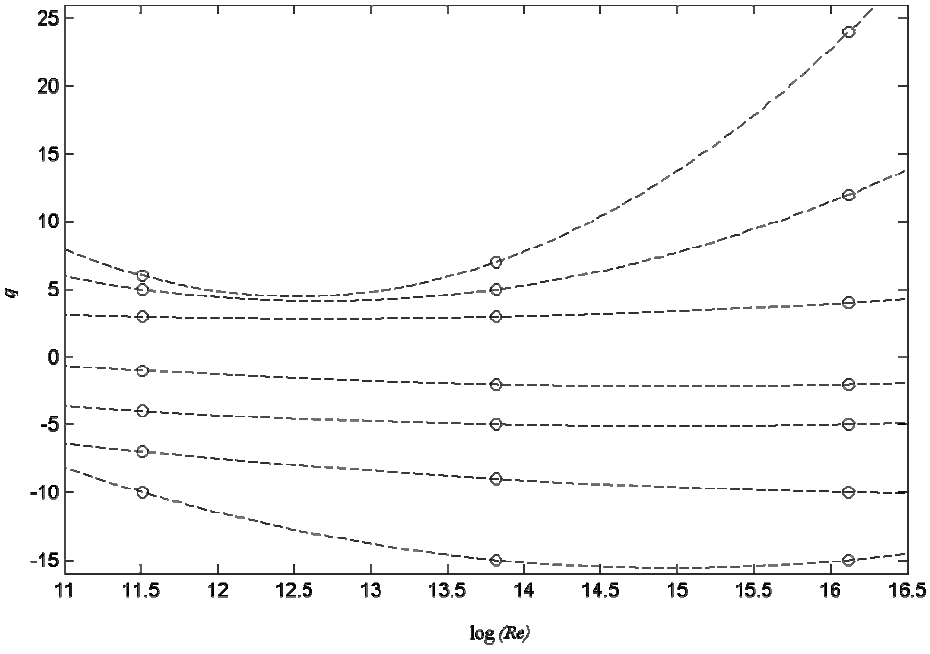

Figure 23. The scaling of cases R2N15, R3N18 and R4N21with scaling factor q.

Figure 24 presents the partition function scaling exponents τ_q, which are obtained from figure 20. In figure 25 they are all plotted in one figure and it can also be seen here, that the case R1N12 differes from the others.

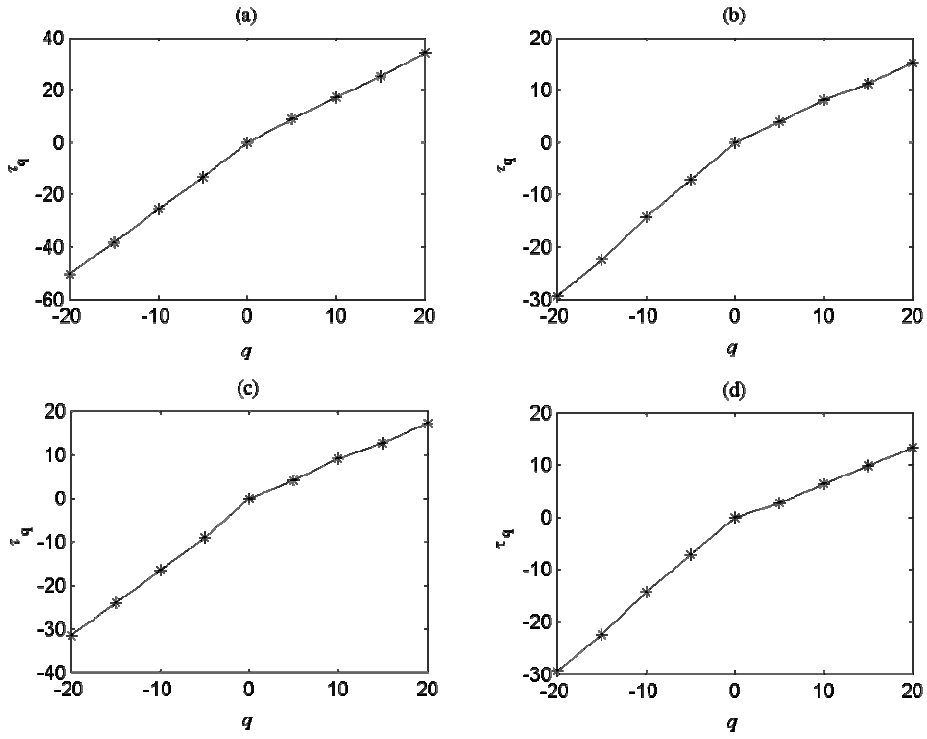

Figure 24. τ_q vs q of cases (a) R1N12, (b) R2N15, (c) R3N18 and (d) R4N21.

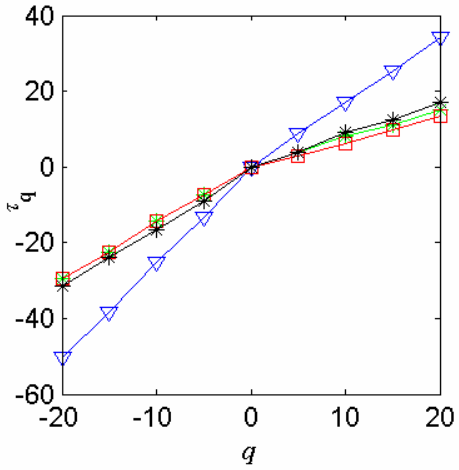

Figure 25. τ_q vs q of cases R1N12 (blue triagle), R2N15 (green asterisk), R3N18 (black asterisk) and R4N21 (red square).

6 CONCLUSIONS

The objective of this thesis was to study the use of wavelets in turbulence applications. Wavelets and their role in modeling and analysis of turbulence were discussed generally. Waveles were used to analyze the intermittency in a turbulence model. The model under study was the GOY (Gledzer 1973, Ohkitani & Yamada 1989) shell model.

The results of this thesis give important information of the nature of the intermittent activities that a turbulence shell model produces. Simulations were performed with varying Reynolds number, shell number and external forcing. Intermittency appears in the model as singular bursts in energy dissipation signal and those bursts were studied for different cases using continuous wavelet transform.

The local scaling exponent α of the wavelet transform describes the character of a singularity. Larger values of α mean more local singularities. The results gave an insight that as Reynolds number increases, the singularities become more local. Varying the shell number at certain Reynolds number affects also the nature of singularities. As the shell number is increased the scaling exponent α gets larger values and the singularities become more local.

Partition function Z gives a measure for intermittency, that is, how frequent the energy dissipation bursts occur. Wavelet coefficients powered with a scaling factor q, are summed over modulus maxima points at each scale. The power q scales the intermittency and makes it possible to compare different cases. The study revealed that at $Re \sim 10^7$ bursts are more frequent than other cases with lower Re. The intermittency of bursts for the cases with $Re \sim 10^6$ and $Re \sim 10^5$ is similar. For the case R1N12 bursts occur after long waiting time in a different fashion so that it cannot be scaled with higher Re. The scaling factors for the cases are provided in chapter 5.3.4. For the case R1N12 different scaling factors presented for lower and higher scales.

7 FUTURE WORK

Shell models produce only temporal fluctuations and ignore spatial intermittency, which is a character of real turbulence. The objective of future work is to transform the chain model to a tree model in the presence of numerous boundary points in order to study both spatial and temporal intermittency in multiphase flows. Wavelets will be used to gain the spatial geometry in shell models.

REFERENCES

1 Ingrid Daubechies, Ten Lectures on Wavelets. ISBN 0-89871-274-2. Philadelf, Pennsylviania 1992.

2 Marie Farge, Wavelet transforms and their applications to turbulence. France.1992.

3 Payman Jalali, Wavelets & applications. Lappeenranta. August 2000.

4 Marie Farge and Kai Schneider, Coherent Vortex Simulations (CVS) A Semi-Deterministic Turbulence Model Using Wavelets. Marseille Cedex, France. Kluwer Acdemic Publishers 2001. Printed in Netherlands.

5 Franc M. White, Fluid Mechanics. Fourth edition. Singapore. The McGraw-Hill Book Co. 1999.

6 Franc M. White, Viscous fluid flow. Fourth edition. Singapore. ISSBN 0-07-069710-8. The McGraw-Hill, Inc. United States of America, 1974.

7 Tenneces & Lumly, A first course in turbulence. Cambridge MA. MIT, 1992.

8 Payman Jalali, Mo Li, Jouni Ritvanen and Pertti Sarkomaa, Intermittency of energy rapid granular shear flows. Chaos Vol. 13, No. 2, June 2003.

9 Siegfried Grossmann and Detlef Lohse, Intermittency in the Navier-Stokes dynamics. Condensed Matter, Federal Republic of Germany, 1992.

10 Graeme Steward, CFD Modelling of Three-Dimensional Turbulent Buoyant Plumes from a Vertical Heated Cylinder. Master's Thesis. Lappeenranta 1999.

11 Marie Farge, Nicholas Kevlahan, Valérie Perrier and Éric Goirand, Wavelets and Turbulence. Proceedings of the IEEE, Vol. 84, NO. 4, 1996.

12 Marie Farge, Kai Schneider and Patrice Abry, Analyzing and compressing turbulent fields with wavelets. ISSN 1626-8334. France, 2002.

13 A. Arneodo and Grasseau and M. Holschneider, Wavelet Transform of multifractals. The American Physical Society, 1988.

14 L. Biferale and R. M. Kerr, Role of inviscid invariants in shell models of turbulence. The American Physical Society, 1995.

15 L. Biferale, A. Lambert, R. Lima and G. Paladin, Transition to chaos in a shell model of turbulence. Physica D, 1994.

16 Luca Biferale, Shell models of the energy cascade in turbulence. Annual Reviews, 2003.

17 R. Benzi, L. Biferale, R. Tripiccione and E. Trovatore, (1+1)-dimensional turbulence. American Institute of physics, 1997.

18 Eric Aurell, Peter Frick and Vladislav Shaidurov, Hierarchical tree-model of 2D-turbulence. Elsevier Science B.V. 1994.

19 Erik Aurell, Emmanuel Dormy and Peter Frick, Binary tree models of high-Reynolds-number turbulence. The American Physical Society, 1997.

20 Fridolin Okkels, Temporal structures in shell models. The American Physical Society, 2001.

21 Y F. Argoul, A. Arneodo, J. Elezgaray and G. Grasseau, Wavelet analysis of the self-similarity of diffusion-limited aggregates and electrodeposition clusters. The American Physical Society, 1990.

22 Piroz Zamankhan, Ali Mazouchi and Pertti Sarkomaa, Some qualitative features of the Couette flow of monodisperse, smooth, inelastic spherical particles. American Institute of Physics, Vol. 71, No. 26, 1997.

23 J. F. Muzy, E. Bacry and A. Arneodo, Wavelets and multifractal formalism for singular signals: Application to turbulence data. The American Physical Society, 1991.

24 Pierre Kestener and Alain Arneodo, Generalizing the wavelet-based multifractal formalism to random vectorial fields: Application to three-dimensional turbulence velocity and vorticity data. The American Physical Society, 2004.

Unreferred materials

1 Kevin Amaratunga and John R. Williams, Sam Quian and John Weiss, Wavelet-galerkin solutions for one-dimensional partial differential equations. U.S.A. John Wileys Sons, Ltd, 1994.

2 Marie Farge, Kai Schneider and Nicholas Devlahan, Non-Gaussianity of coherent vortex simulation for two-dimensional turbulence using an adaptive orthogonal wavelet basis. American Institute of Physics, 1999.

3 Donoho, D., Unconditional bases are optimal bases for data compression and statistical estimation. Appl. Comput. Harmon. Anal. 1/100, 1993.

4 Donoho, D. and Johnstone, I., Ideal spatial adaption via wavelet shrinkage. Biometrica 81/425-455, 1994.

5 Jens Eggers and Siegfried Grossmann, Anomalous turbulent velocity scaling from the Navier-Stokes equation. Elsevier Science Publischers B. V. 1991.

6 Juhani Suihkonen, Turbulenttisen putkivirtauksen numeerinen mallinnus. Diplomityö. Lappeenrannan teknillinen korkeakoulu. Lappeenranta. 1999.

7 Bhavic R. Bakshi and George Stephanopoulos, Wave-Net: Multiresolution, Hierarchial Neutral Network with Localized Learning. January 1993.

8 Sam Qian and Weiss, Wavelets and the Numerical Solution of Partial Differential Equations. Academic Press, Inc. 1993.

9 Oleg V. Vasilyev, Samuel Paolucci, and Mihir Sen, A Multilevel Wavelet Collocation Method for Solving Partial Differential Equations in Finite Domain. Academic Press, Inc. 1995.

10 Oleg V. Vasilyev and Samuel Paolucci, A Dynamically Adaptive Multilevel Wavelet Collaction Method for Solving Partial Differential Equations in a Finite Domein. Academic Press, Inc, 1996.

11 Roger Temam, Multilevel Methods for the Simulation of Turbulence, A Simple Model. Academic Press, Inc, 1996.

12 R. L. Schult and H. W. Wyld, Using wavelets to solve the Burgers equation: A comparative study. The American Physical Society 1992.

13 Center for Multiphase Flows Research, Numerical simulation of dilute turbulent gas-solid flows. S.K.K Lun. Elsevier Science Ltd. 2000.